Chronic interstitial nephritis in agricultural communities is a toxin-induced proximal tubular nephropathy

see commentary on page 258

OPEN

Benjamin A. Vervaet[1], Cynthia C. Nast[2], Channa Jayasumana[3], Gerd Schreurs[1], Frank Roels[4], Chula Herath[5], Nika Kojc[6], Vahid Samaee[7], Sonali Rodrigo[5], Swarnalata Gowrishankar[8], Christiane Mousson[9], Rajeewa Dassanayake[10], Carlos M. Orantes[11], Vincent Vuiblet[12], Claire Rigothier[13], Patrick C. D'Haese[1] and Marc E. De Broe[1]

[1]Laboratory of Pathophysiology, University Antwerp, Antwerp, Belgium; [2]Cedars-Sinai Medical Center, Los Angeles, California, USA; [3]Faculty of Medicine, Rajatrata University of Sri Lanka, Anuradhapura, Sri Lanka; [4]Department of Pathology, Ghent University, Gent, Belgium; [5]Department of Nephrology, Sri Jayewardenepura General Hospital, Colombo, Sri Lanka; [6]Institute of Pathology, Faculty of Medicine, University of Ljubljana, Ljubljana, Slovenia; [7]Electron Microscopy for Materials Science (EMAT), University of Antwerp, Antwerp, Belgium; [8]Department of Pathology, Apollo Hospitals, Hyderabad, India; [9]Department of Nephrology, Centre Hospitalier Universitaire de Dijon, Dijon, France; [10]Renal Unit, General Hospital, Polonnaruwa, Sri Lanka; [11]National Institute of Health, Ministry of Health of El Salvador, San Salvador, El Salvador; [12]Departments of Nephrology and Renal Pathology, Centre Hospitalier Universitaire de Reims, Reims, France; and [13]Service Néphrologie, Transplantation, Dialyse et Aphérèses, Centre Hospitalier Universitaire de Bordeaux, Bordeaux, France

Almost 30 years after the detection of chronic interstitial nephritis in agricultural communities (CINAC) its etiology remains unknown. To help define this we examined 34 renal biopsies from Sri Lanka, El Salvador, India and France of patients with chronic kidney disease 2-3 and diagnosed with CINAC by light and electron microscopy. In addition to known histopathology, we identified a unique constellation of proximal tubular cell findings including large dysmorphic lysosomes with a light-medium electron-dense matrix containing dispersed dark electron-dense non-membrane bound "aggregates". These aggregates associated with varying degrees of cellular/tubular atrophy, apparent cell fragment shedding and no-weak proximal tubular cell proliferative capacity. Identical lysosomal lesions, identifiable by electron microscopy, were observed in 9% of renal transplant implantation biopsies, but were more prevalent in six month (50%) and 12 month (67%) protocol biopsies and in indication biopsies (76%) of calcineurin inhibitor treated transplant patients. The phenotype was also found associated with nephrotoxic drugs (lomustine, clomiphene, lithium, cocaine) and in some patients with light chain tubulopathy, all conditions that can be directly or indirectly linked to calcineurin pathway inhibition or modulation. One hundred biopsies of normal kidneys, drug/toxin induced nephropathies, and overt proteinuric patients of different etiologies to some extent could demonstrate the light microscopic proximal tubular cell changes, but rarely the electron microscopic lysosomal features. Rats treated with the calcineurin inhibitor cyclosporine for four weeks developed similar proximal tubular cell lysosomal alterations, which were absent in a dehydration group. Overall, the finding of an identical proximal tubular cell (lysosomal) lesion in CINAC and calcineurin inhibitor nephrotoxicity in different geographic regions suggests a common paradigm where CINAC patients undergo a tubulotoxic mechanism similar to calcineurin inhibitor nephrotoxicity.

Kidney International (2020) **97,** 350–369; https://doi.org/10.1016/j.kint.2019.11.009

KEYWORDS: agrochemicals; calcineurin inhibition; CKD lysosomes; diagnosis; proximal tubule

In the last decade of the 20th century, alert clinicians in Central America and Sri Lanka described a large number of patients in their rural agricultural communities with relatively rapidly progressive chronic kidney disease (CKD) without hypertension or diabetes. Males were predominantly affected, including sugar cane workers in Central America and paddy farmers in Sri Lanka.[1] In Central America the disease was named "Meso-American Nephropathy" (MeN), whereas in Sri Lanka, "CKD of unknown etiology" (CKDu) was the prefered terminology. In light of the comparable clinical, pathological, and epidemiological expression of the disease, the term Chronic Interstitial Nephritis in Agricultural Communities (CINAC) was proposed to describe both entities.[2] Classic presentations of CINAC are young men, primarily agricultural workers, with common socioeconomic and occupational determinants including a hot tropical climate, poverty, and exposure to potentially toxic agrochemicals through ingestion of contaminated food, drinking water from shallow contaminated wells, inhalation, and (in)

Correspondence: *Benjamin A. Vervaet or Marc E. De Broe, Universiteitsplein 1, 2610 Antwerp, Antwerp, Belgium. E-mail: benjamin.vervaet@uantwerpen.be or marc.debroe@uantwerpen.be*

Received 17 May 2018; revised 9 September 2019; accepted 10 October 2019; published online 23 November 2019

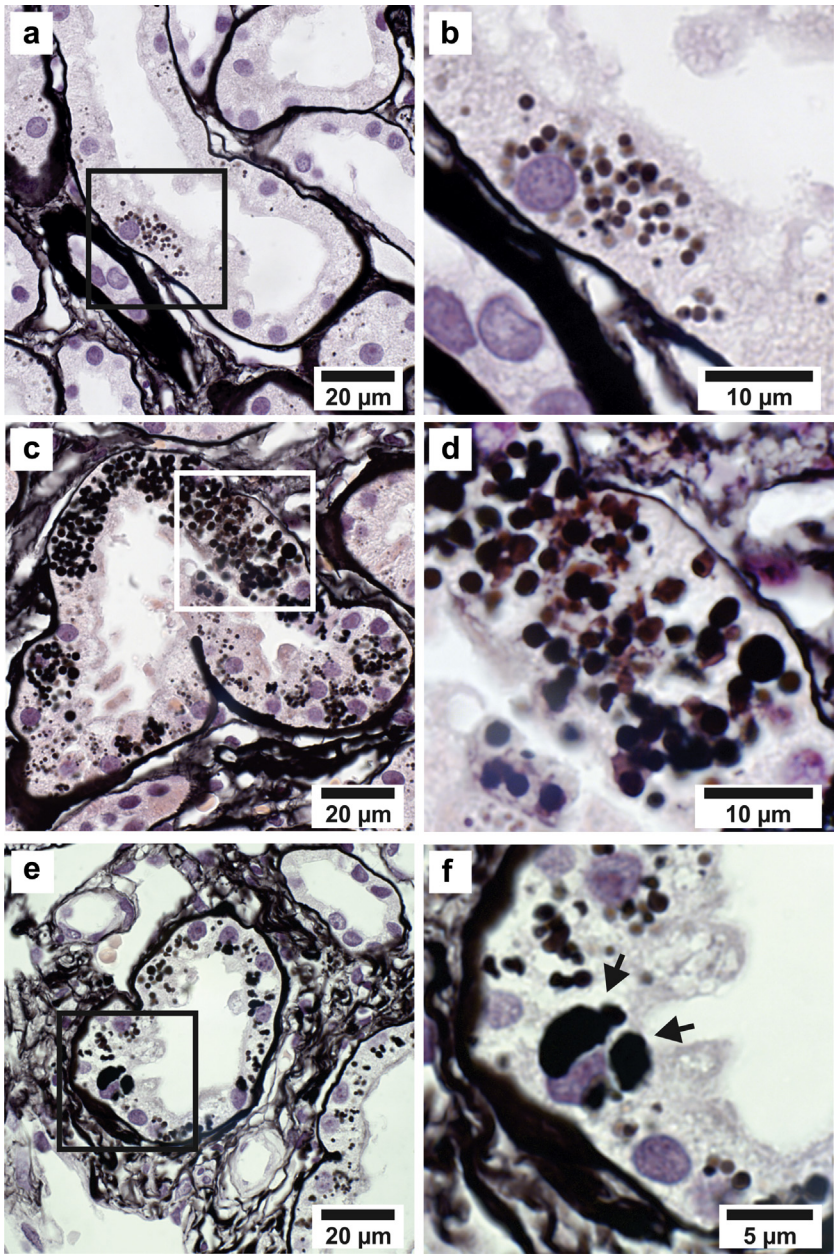

Figure 1 | Jones-stained sections revealed prominent accumulation of intracellular granules with different phenotypic appearances. Mild accumulations not affecting every cell of the tubular profile (**a,b**). Extensive intracellular accumulation of enlarged granules (**c,d**). Prominent enlarged granules, some with irregular/dysmorphic shapes (arrows; **e,f**). Images from the Sri Lankan Chronic Interstitial Nephritis in Agricultural Communities cohort. To optimize viewing of this image, please see the online version of this article at www.kidney-international.org.

direct skin contact. CINAC cases also have been identified among less exposed individuals including nonagricultural workers, women, and children who live in the same tropical environment.[3] Recent reports suggest that similar patterns of CKD may occur in the Uddanam region of Andhra Pradesh in India, Egypt, Tunisia, Senegal, and very recently in Peru.[4] Clinically, CINAC is characterized by absent or low tubular proteinuria, CKD stages 3 to 4, small kidneys with irregular contours on imaging, and without traditional causes of CKD, such as glomerulonephritis, diabetes, and hypertension. Renal biopsies show varying degrees of tubular atrophy, interstitial fibrosis, interstitial inflammation, and glomerulosclerosis.[5,6] The progression of renal disease is relatively rapid, with end-stage renal failure occurring over 4 to 10 years. However, no specific/sensitive "signature" lesions have been found to date to define CINAC and differentiate it from other chronic renal diseases.

Two primary triggers have been proposed: toxic exposures in the agricultural communities and heat stress with repeated episodes of dehydration causing recurrent acute kidney injury leading to CKD. The dehydration hypothesis,

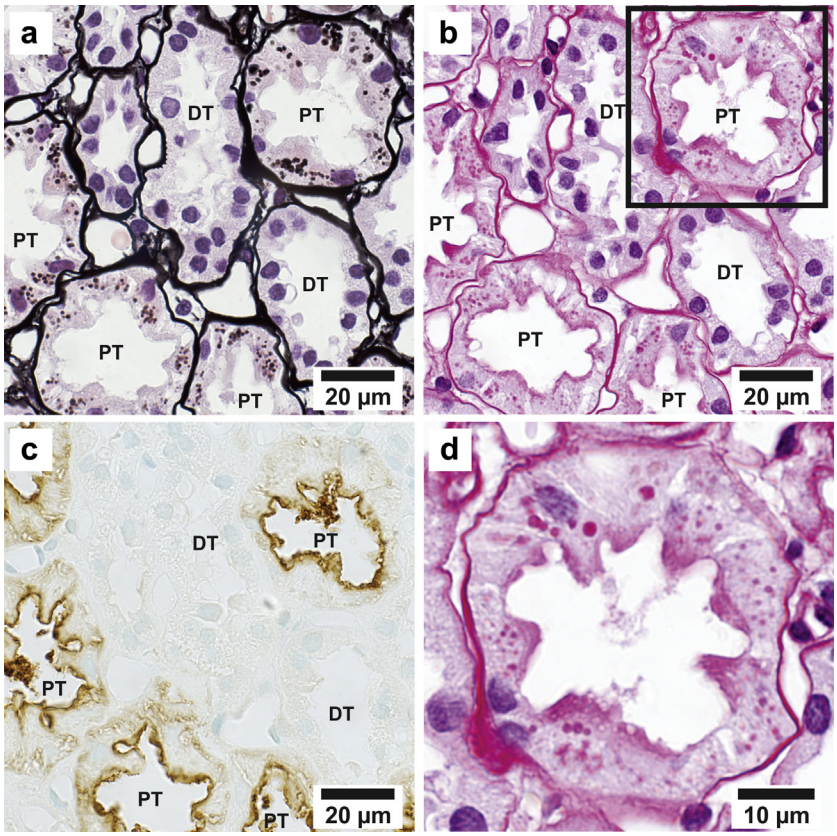

Figure 2 | Accumulation of granules is confined to the proximal tubular epithelium. Jones-stained section (**a**) serial to a periodic acid–Schiff (PAS)–stained section (**b**) reveals that the affected proximal tubules (PTs) contain brush border or brush border remnants. Section serial to (**a**) stained for the proximal epithelial marker gamma-glutamyltranspeptidase 1 (**c**). Detail of (**b**) showing intracellular PAS-positive granules, resembling those found in the Jones stain, is shown in (**d**). DT, distal tubule. Images from the Sri Lankan Chronic Interstitial Nephritis in Agricultural Communities cohort. To optimize viewing of this image, please see the online version of this article at www.kidney-international.org.

however, cannot explain why the incidence of CINAC has increased in association with the increased use of agrochemicals in paddy farming in the 1990s, why CINAC is absent in hotter northern Sri Lanka, Cuba, and Myanmar where agrochemicals are rarely used, why there is a mosaic geographical pattern in CINAC endemic areas, why CINAC occurs in women, children, and adolescents who are not agricultural workers, and why there are extrarenal manifestations of CINAC.[2,7] Heat stress and dehydration may be contributory risk factors to disease development but cannot be assigned an isolated causal role in the development of CINAC.

Here we present compelling evidence that CINAC is a lysosomal tubulopathy likely caused by a toxic substance or substances.

RESULTS

Patients with CINAC demonstrate accumulation of proximal tubular cell cytoplasmic granules

All patients with CINAC were selected based on current clinical criteria.[2] Periodic acid–Schiff and Jones stained renal biospy sections demonstrated the classic histopathologic features associated with CINAC at all 4 locations[2,6,8,9]: varying extents of tubular atrophy, tubulointerstitial fibrosis (sometimes striped), inflamed fibrosis, glomerulosclerosis, glomerulomegaly, and vascular hyalinosis/sclerosis (Supplementary Figure S1 and Supplementary Table S1). None of the biopsies showed evidence of uric acid deposition on hematoxylin and eosin stain or electron microscopy (EM).

Jones staining revealed accumulations of silver positive light brown to black cytoplasmic granules in cortical tubular cells (Figure 1). These granules, optimally observed at magnifications ≥400×, varied in size from finely granular to prominent (≥ one-third of nuclear size), with discrete borders and a round to irregular/dysmorphic shape (Figure 1b, d, and f; Supplementary Figure S2). Tubular profiles ranged from unaffected to heavily involved, and affected tubular cells had few to several dozen granules observed on 2- to 4-µm sections (Figure 1).

Serial sections stained with Jones, periodic acid–Schiff, and gamma-glutamyltranspeptidase 1, respectively, showed that the intracellular granules were confined to proximal tubule (PT) segments, including S1, S2, S3 (Figure 2; Supplementary Figure S3). These argyrophyllic granules were not found in distal tubules, identified by more closely apposed and

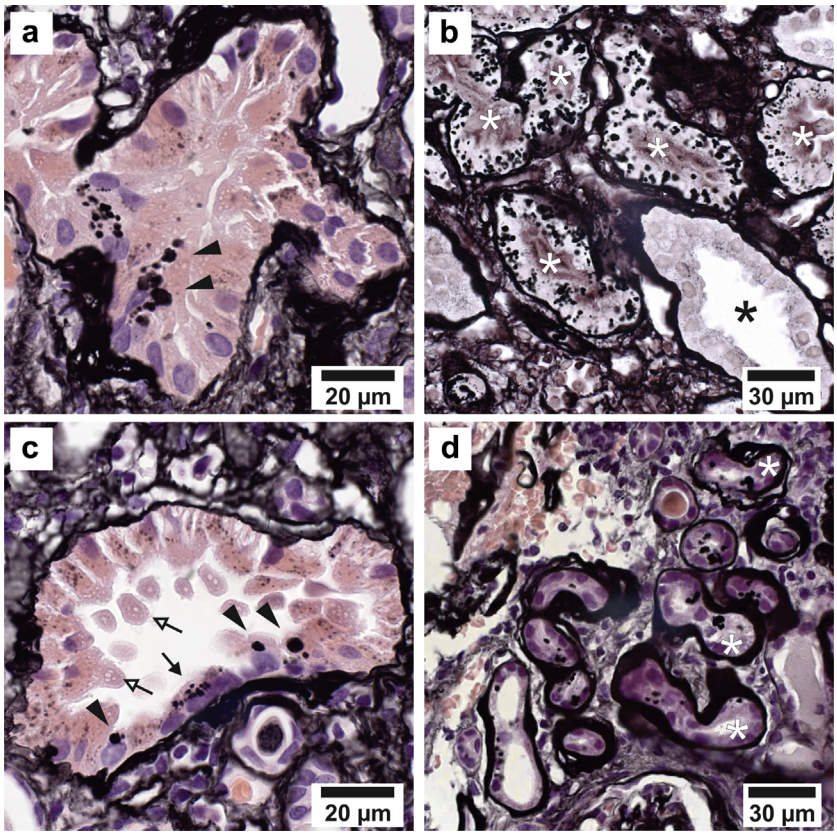

Figure 3 | Histopathological phenotypes of granule-containing proximal tubular epithelia observed on Jones-stained tissue sections. Proximal epithelium with conserved epithelial height, focally containing enlarged argyrophyllic granules (arrowheads; **a**). White asterisks depict atrophic tubuli, containing many enlarged granules, with thickened basement membranes in a fibrotic area (**b**). The black asterisk identifies an unaffected distal tubule. Affected tubuli demonstrating enlarged granules (arrowheads), flattened atrophic epithelial cells with loss of brush border (solid arrow), and apical blebbing and cell fragment shedding (open arrows; **c**). Prominent atrophy of tubules with enlarged granules, thickened basement membranes and expanded interstitial compartment (**d**). Images (**a**), (**c**), and (**d**) are from the Sri Lankan Chronic Interstitial Nephritis in Agricultural Communities cohort; image (**b**) is from an Indian patient. To optimize viewing of this image, please see the online version of this article at www.kidney-international.org.

cuboidal epithelial cells and absence of apical brush border (Figure 2a and b).

Histopathology of the PT epithelium in patients with CINAC

PT cells (PTCs) containing large argyrophilic granules had a variety of appearances ranging from preserved height to flattening and simplification with and without loss of brush border in a diffuse to focal distribution (Figure 3). Focally, PTCs had apical blebs, with and without silver positive granules, protruding into the tubular lumen (Figure 3c; Supplementary Figure S4). These membrane-bound fragments appeared to shed in the lumen, although tangential cutting must be considered (Figure 3c; Supplementary Figure S4). Atrophic tubules often but not always were more likely to contain enlarged argyrophilic granules, although they also could be seen in preserved tubulointerstitial areas. Affected PTCs had a nonproliferative, nonapoptotic phenotype, in contrast to distal tubular cells (Figure 4[10,11]).

Autofluorescence of intracellular PTC granules in patients with CINAC

PTC granules in patients with CINAC demonstrated autofluorescence clearly contrasting with the cellular background (Figure 5). Comparing the same deparaffinized renal tissue section with autofluorescence and after Jones staining demonstrated that almost all autofluorescent granules were argyrophylic (Figure 5).

Proximal epithelial intracellular granules in patients with CINAC are lysosomes

Staining of serial sections demonstrated cathepsin B–positive granules in PTCs with argyrophylic granules (Figures 5b and 6a). Immunofluorescent staining for cathepsin B followed by Jones staining on the same slide revealed the that cathepsin B–positive lysosomes are argyrophylic (Figure 6c and d). The same strategy with a nuclear marker (PCNA) did not result in argyrophylic nuclei, demonstrating specificity of the Jones reaction for lysosomes (data not shown). In patients with CINAC, autofluorescent granules were further characterized by staining for cytochrome c oxidase subunit 6C (COX6C), lysosomal associated membrane protein 1 (LAMP1), and cathepsin B. COX6C was absent in affected tubules, making it unlikely that the autofluorescent/argyrophylic granules are mitochondria, and may indicate injured/dysfunctional

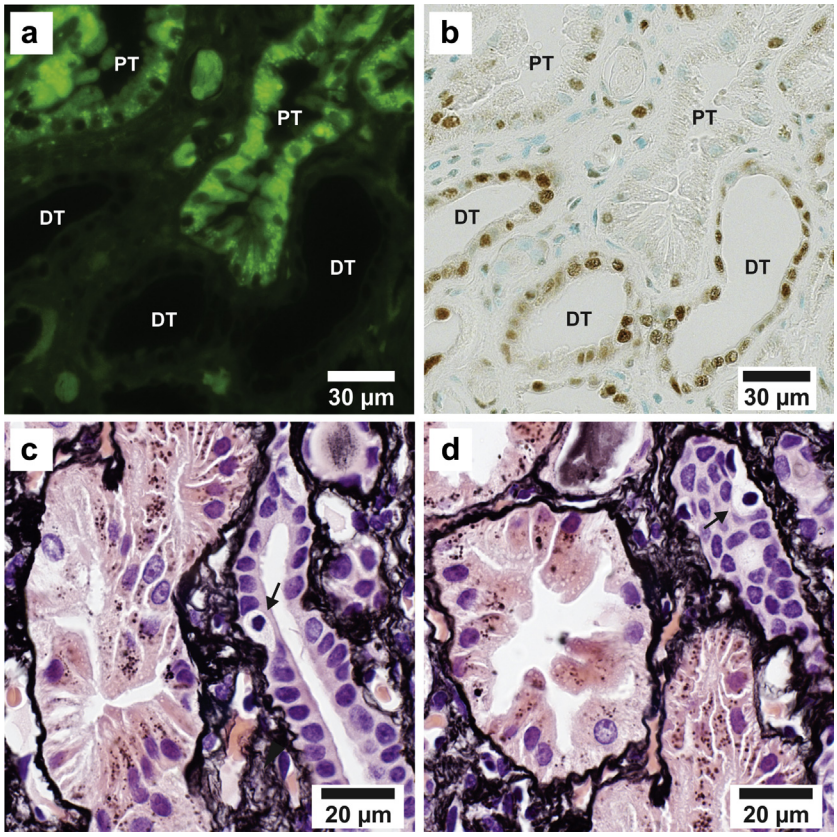

Figure 4 | Proximal tubules (PTs) with lysosomal accumulation have minimal to no proliferative activity or apoptosis. Autofluorescence revealing Chronic Interstitial Nephritis in Agricultural Communities (CINAC)–affected proximal tubules (**a**). The same section as in (**a**) stained for the proliferation marker proliferating cell nuclear antigen (**b**). There were very few scattered proliferating epithelial cells in the affected PTs; in contrast, distal nephron cells demonstrated prominent proliferative activity. In 25% of distal tubules (DTs), the proliferative distal tubular epithelium has scattered apoptotic cells (arrows) as evidenced by the typical condensed nuclei surrounded by a bright halo on hematoxylin and eosin counterstain[10,11] (**c,d**). Apoptosis was not present in PT cells. Images (**a**) and (**b**) are from a patient with CINAC from El Salvador. Images (**c**) and (**d**) are from a patient with CINAC from Sri Lanka. To optimize viewing of this image, please see the online version of this article at www.kidney-international.org.

mitochondria (Supplementary Figure S5). Confocal microscopy with LAMP1 and cathepsin B staining identified an important subset of the granules as lysosomes (Figure 7; Supplementary Figure S6). Additional staining for enzymatic activity of lysosomal enzyme acid phosphatase revealed a granular pattern in tubules with autofluorescent granules (Supplementary Figure S7).

Proximal epithelial lysosomes in patients with CINAC have an aberrant ultrastructural phenotype

EM revealed that PTCs in patients with CINAC focally contain few to many large inclusions delineated by a single (often indistinctive) membrane (Figure 8a and b; Supplementary Figure S8). The inclusions lacked cristae or other features of mitochondria, autophagic vacuoles, lipofuscin/ceroid droplets, or peroxisomes (marginal plate) but were consistent with lysosomes.[12–16] The EM appearance corresponded to argyrophylic lysosomes on Jones stained slides (Figure 8c–e). Transmission EM energy-dispersive x-ray spectroscopy on EM grids prepared from Jones stained 3-µm sections confirmed the presence of Jones-stain derived silver (Ag) and gold (Au) atoms specifically in the intracellular inclusions, thereby linking light microscopy (LM) to EM morphology and corroborating the lysosomal nature of the inclusions (Figure 9).

These lysosomes were mildly to markedly larger than mitochondria, often with irregular/dysmorphic, sometimes very distorted, shapes (Figure 10a and b). The longest diameter was 5.3 µm, and the average longest diameter of the 140 largest lysosomes from the Sri Lanka CINAC cohort was 1.75 ± 0.69 µm, larger than the normal lysosomal diameter of 0.1 to 1.0 µm (Supplementary Figure S9).[17,18]

Nearly all enlarged/dysmorphic lysosomes contained homogenous, nonmembrane bound, dark electron dense rounded/irregular "aggregates" dispersed throughout the lysosomal matrix, which was of light to medium uniform electron density; a small percentage of lysosomes additionally contained dark electron dense punctate material (Figures 8 and 10). The CINAC lysosomes did not resemble lysosomal meyloid bodies because no lamellar pattern was observed in any enlarged lysosomes.[19–22] Also, CINAC

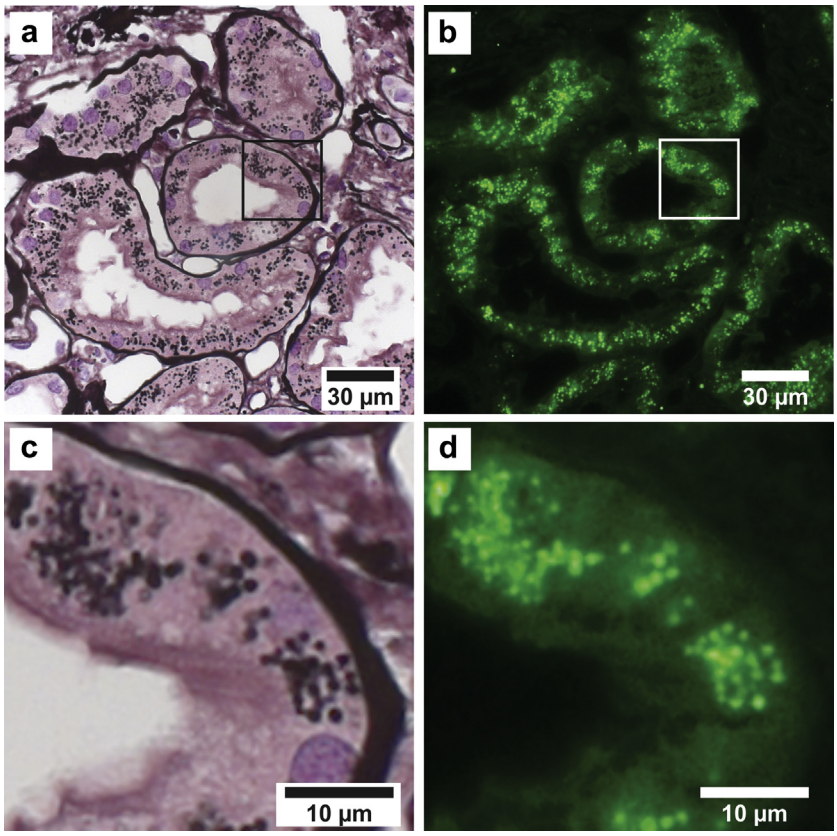

Figure 5 | Granules displaying autofluorescence are silver-positive on Jones stain. To demonstrate this phenomenon, autofluorescence was first digitized (**b,d**), followed by Jones staining on the same tissue section (**a,c**). Images are from a patient with Chronic Interstitial Nephritis in Agricultural Communities from El Salvador. To optimize viewing of this image, please see the online version of this article at www.kidney-international.org.

lysosomes are not to be mistaken for degenerating mitochondria, which can contain swollen dark electron dense cristae (Supplementary Figure S10). In addition, cases with large dysmorphic lysosomes typically contained clusters of at least 3 smaller (<1.2 µm in greatest dimension) lysosomes, with the same features as their larger counterparts (Figure 10c and d). The CINAC lysosomal diagnostic criteria are provided in Table 1.

Specificity and sensitivity of the proximal tubular epithelial lesions

To determine whether the PTC lesion is specific for CINAC, we analyzed renal biopsy specimens from healthy control subjects ($n = 10$), from patients with CINAC from Sri Lanka ($n = 18$), El Salvador ($n = 11$), India ($n = 1$), and France ($n = 4$), 5 proteinuric nephropathies ($n = 16$), non-CINAC Sri Lankan glomerulopathies ($n = 6$), interstitial nephritis ($n = 19$), and 6 drug/toxin-induced nephropathies, including calcineurin inhibitor treatment ($n = 49$; Tables 2 and 3). All were evaluated by Jones stained LM sections and EM.

Of the 32 CINAC biopsies with EM, 26 (81.3%) contained the dysmorphic lysosomal phenotype (Table 2 and Figure 11). EM analysis of healthy and pathologic control conditions revealed that the CINAC-lysosomal phenotype occurred in a substantial number of renal transplant indication biopsies on calcineurin inhibitor (CNI) therapy (79%), lithium exposure (78%), light chain disease (40%), drug-induced interstitial nephritis (27%), and in cases of lomustine, clomiphene, and rarely tenofovir nephrotoxicity (Table 3, Figure 12, and Supplementary Figure S11). Healthy and proteinuric control subjects rarely had the EM lysosomal lesion. The intralysosomal electron-dense structures appear slightly coarser in CINAC cases compared with CNI exposure, yet the overall morphology is the same (Supplementary Figure S12). In contrast, PTC lysosomes from patients with moderate or overt proteinuria, not living in CINAC endemic regions, were round to occasionally irregular, with variably electron-dense matrix, and no to various filamentous, lipidlike, or aggregated contents, but lacking the specific structure of the CINAC lysosomes (Figure 13). The vast majority of our CINAC cohort lacked moderate or overt proteinuria (Table 2). Two Sri Lankan patients with CINAC had type 2 diabetes, and one was positive for the dysmorphic lysosomal lesion (Table 2).

By LM, patients with CINAC demonstrated PTC argyrophylic granules, epithelial simplification, blebbing, and cell fragment shedding in focal/diffuse patterns. All non-CINAC

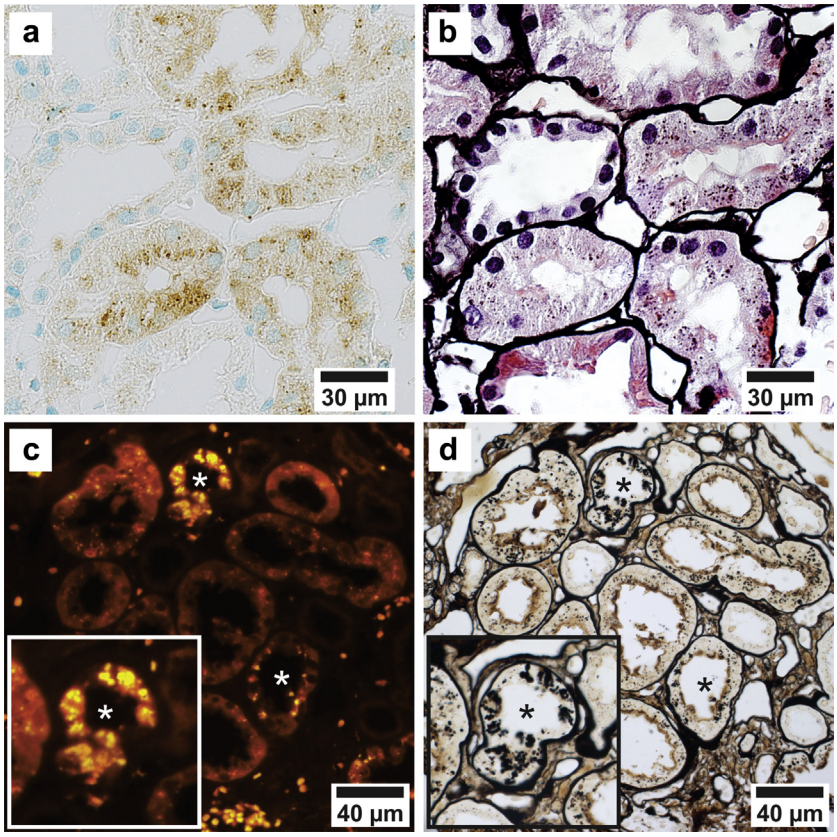

Figure 6 | Enlarged intracellular granules are lysosomes. Serial section (**a**) to (**b**) demonstrating granular immunopositivity for the lysosomal marker cathepsin B in tubules that contain Jones-positive granules (**b**). Immunofluorescent staining for cathepsin B demonstrating enlarged lysosomes in several tubuli (white asterisks; **c**). Jones staining (**d**) on the section displayed in (**c**) revealed that the same lysosomes are argyrophyllic (black asterisks). Images (**a**) and (**b**) are from a patient with Chronic Interstitial Nephritis in Agricultural Communities (CINAC) from El Salvador. Images (**c**) and (**d**) are from a Sri Lankan patient with CINAC. To optimize viewing of this image, please see the online version of this article at www.kidney-international.org.

cohorts, occasionally to regularly, presented PTC normal-sized argyrophylic granules (<1 μm). However, enlarged argyrophylic lysosomes (greater than one-third of nuclear size) with associated tubular atrophy tended to be predictive of the lysosmal lesion on EM.

The PT lysosomal lesion is an acquired phenotype

The presence of the aberrant lysosomal lesion in patients treated with CNI prompted us to include a transplant protocol biopsy cohort, a unique clinical setting allowing us to evaluate whether implantation biopsies (normal kidneys of living/deceased donors) show the aberrant lysosomes and whether patients develop them during the course of their subsequent CNI therapy. On EM, the diagnostic lysosomes were observed in 9% (3 of 35), 50% (5 of 10), and 67% (6 of 9) of renal transplant protocol biopsy speciments taken at implantation, and after 6 and 12 months of CNI therapy, respectively (Figure 14). The lesion was found in 76% (16 of 21) of indication biopsies from patients taking CNIs (Figure 14). It is worthwhile to note that the lysosomal lesion in protocol biopsies was found in the absence of decreased renal function (data not shown).

Etiology of the CINAC specific lesion: rat study

LM of cyclosporine-treated rat kidneys showed PTC injury characterized by focal flattening and early tubular atrophy (Figure 15c). Focally, PTCs contained enlarged argyrophilic and autofluorescent granules (Figure 15c and h; Supplementary Figures S13 and S14), which were identified as lysosomes by Lysosomal Associated Membrane Protein 1 (LAMP1) staining (Figure 16). In control and dehydrated rats, PTCs contained fewer argyrophilic and autofluorescent granules and no PTC damage (Figure 15a, b, d, and f; Supplementary Figures S13 and S14). No groups had glomerulosclerosis or inflammation. By EM, dehydrated and control animals had a variety of lysosomal appearances; however, none had the large dysmorphic lysosomes found in patients with CINAC (Figure 15e and g). In contrast, dysmorphic large lysosomes were found focally in PTCs of the cyclosporine-treated animals, although intralysosomal

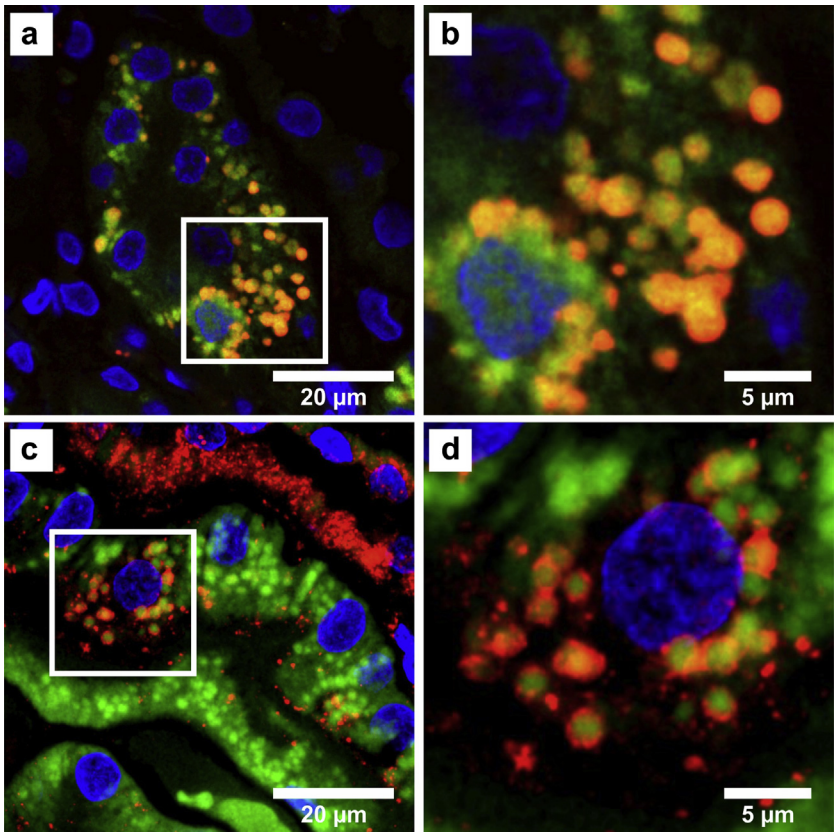

Figure 7 | Autofluorescent granules are lysosomes. Confocal microscopy of red-stained cathepsin B demonstrating that a subset of the enlarged green autofluorescent granules are positive for this lysosomal enzyme (**a**). Detail of (**a**) is shown in (**b**). Confocal microscopy of red-stained lysosomal-associated membrane protein 1 demonstrating that a subset of the enlarged green autofluorescent granules are delineated by this lysosomal membrane marker (**c**). Detail of (**c**) is shown in (**d**). Images are from a Sri Lankan patient with Chronic Interstitial Nephritis in Agricultural Communities. To optimize viewing of this image, please see the online version of this article at www.kidney-international.org.

electron-dense aggregates were not observed (Figure 15). Body weight, renal function, urinary osmolality, and protein excretion are available in the Supplementary Data.

DISCUSSION

This study is the first to formally demonstrate a lysosomal proximal tubulopathy, characterized by enlarged dysmorphic lysosomes containing dispersed aggregates, in association with varying degrees of epithelial atrophy, apparent cell fragment shedding, and weak to no PTC proliferative capacity, in patients from Sri Lanka, El Salvador, India, and France with the clinical diagnosis of CINAC. A similar lysosomal lesion was identified in patients treated with the CNIs cyclosporine and tacrolimus, in several drug/toxin-related nephropathies and in a subset of patients with light chain tubulopathy. Experiments in rats demonstrated that dehydration/heat stress over 4 weeks does not induce this lysosomal lesion. In contrast, PTC lysosomes approaching the aberrant phenotype were found after administration of cyclosporine. Evaluation of implantation and protocol biopsy specimens (taken at 6 and 12 months of CNI use) revealed that the lysosomal phenotype is acquired in association with CNI exposure. In view of the inherent nephrotoxicity of CNIs and the documented CNI effect of herbicides/insecticides used/abused by patients with CINAC, this lysosomal tubulopathy provides evidence that CINAC is the pathologic expression of a toxic insult.[23–28] Currently it is not clear if the abnormal lysosomes are intrinsically injurious or merely markers of toxicity.

During the past 30 years, CINAC/CKDu/MeN emerged in different parts of the world and is now reaching alarming numbers globally.[2] Our finding that the PTC aberrant lysosomes are present in such patients from 4 (tropical and nontropical) locations corroborates the global scale and strongly suggests that this proximal tubulopathy shares a common etiology independent of the endemic region. Moreover, the identification of one patient with CINAC who had type 2 diabetes supports the supposition that CINAC likely is superimposable. However, several factors impede the prevention and treatment of this nephropathy; the etiology/pathophysiology is unknown, only clinically nonspecific criteria are available, and biopsies are nondiagnostic. This study provides new insights into these issues.

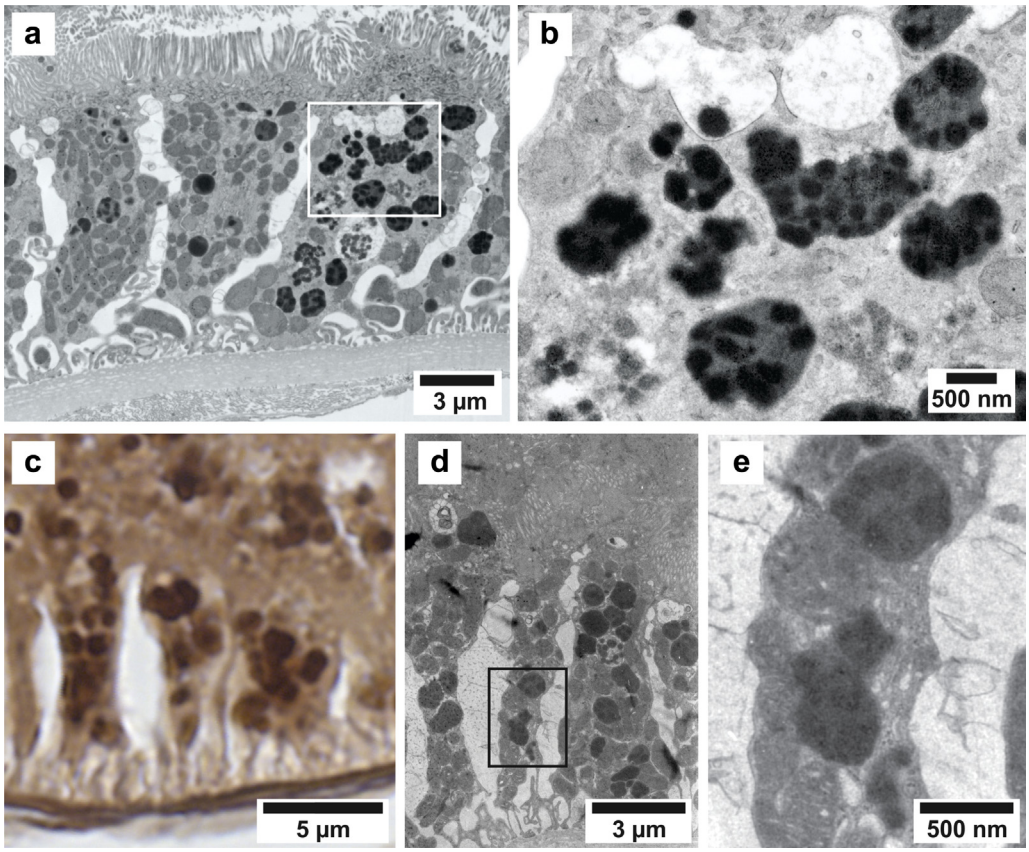

Figure 8 | Transmission electron microscopic (EM) analysis revealed the presence of distinct proximal tubular single membrane–bound inclusions (lysosomes) in patients with Chronic Interstitial Nephritis in Agricultural Communities (CINAC). Low-magnification overview demonstrating several cells with the accumulation of enlarged lysosomes (**a**). High-magnification detail of (**a**) demonstrating dysmorphic lysosomes containing dark electron-dense aggregates (**b**). The EM appearance of the lysosomes is concordant with the cytoplasmic lysosomes observed on Jones-stained sections (**c–e**). High magnification of affected epithelial cells on Jones stain (**c**). EM image of a similar region as (**c**) is shown in (**d**). Higher magnification of (**d**) showing the medium electron-dense matrix containing dispersed electron-dense aggregates (**e**). Images from Sri Lankan patients with CINAC. To optimize viewing of this image, please see the online version of this article at www.kidney-international.org.

To determine the diagnostic sensitivity/specificity of the abnormal lysosomes, we analyzed renal biopsy specimens from healthy control subjects and from several proteinuric, toxin-induced, and other nephropathies. We identified a similar PTC lysosomal lesion in patients who had and had not received transplants and were treated with CNIs, in patients exposed to lithium, in subsets of patients with drug-induced interstitial nephritis and light chain tubulopathy, and in cases of lomustine, clomiphene, and rarely tenofovir nephrotoxicity. Studies of cyclosporine exposure in rats and humans have incidently reported inclusion bodies in renal tubular cells, which were identified by EM as enlarged (auto)lysosomes.[29–33] Additionally, atrophied PT epithelium in cyclosporine-treated rats has been reported to contain large lysosomes by acid phosphatase immunostaining.[34] Here, these enlarged lysosomes are characterized by EM in humans as dysmorphic and containing dispersed dark intralysosomal aggregates. Surprisingly, and to the best of our knowledge, this lysosomal abnormality has not been explored previously as a marker or mechanism of CNI nephrotoxicity. In some patients with light chain disease and proximal tubulopathy with lysosomal "indigestion/constipation,"[35,36] a portion of the PT lysosomes appear dysmorphic, similar to those in patients with CINAC. To the best of our knowledge, this lysosomal lesion in the previously listed drug/toxin-related nephropathies has never been reported clearly. The striking morphologic similarity thereof, together with patients who have CINAC, patients treated with CNI, and patients with light chain tubulopathy, strongly suggests a common etiologic process and/or underlying mechanism.

CNIs prolong graft survival and can be effective in immune-related diseases, but all have known nephrotoxic effects.[37–40] A study of 61 cyclosporine analogues showed that nephrotoxicity correlated with the immunosuppressive activity of the analogues, demonstrating that CNI actions are profoundly associated with toxic injury.[40] The similarity of the lysosomal phenotype in patients with CINAC and in patients treated with CNIs strongly suggests that CINAC is a toxin-induced nephropathy

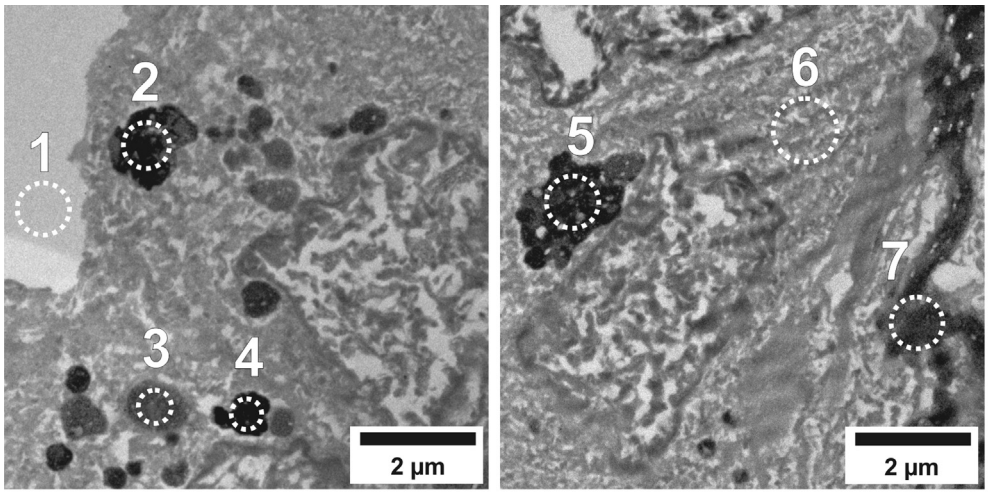

Region	Description	Atomic% Ag	Atomic% Au
1	Outside tissue	0	0
2	Large dysmorphic lysosome	0.37	1.64
3	Round lysosome	0.89	1.98
4	Small dysmorphic lysosome	0.44	1.80
5	Large dysmorphic lysosome	0.43	1.47
6	Cytoplasm	0.007	0
7	Basement membrane	1.03	4.5

Figure 9 | Transmission electron microscopy (EM)–energy dispersive x-ray analysis confirmed, on the ultrastructural level, that lysosomes (either enlarged/dysmorphic or not) are argyrophylic. Pictures are EM grids prepared from Jones-stained 3-µm sections. Numbered regions depict electron-beam exposure for elemental analysis. The table shows the atomic percentage of silver (Ag) and gold (Au), which are derived from the Jones staining. Lysosomes contained increased amounts of Ag and Au, as did the basement membrane (region 7) that is known for its argyrophylic properties. Images are from a patient with Chronic Interstitial Nephritis in Agricultural Communities from El Salvador. To optimize viewing of this image, please see the online version of this article at www.kidney-international.org.

(Supplementary Table S2[6,41–44]). Additionally, Bolzoni *et al.*[45] reported that multiple myeloma cells are able to inhibit noncanonical Wnt5a, an upregulator of calcineurin, suggesting that myeloma cells may have CNI effects, explaining the lysosomal phenotype in selected patients with light chain disease. Furthermore, clomiphene, lomustine, lithium, and cocaine have been reported to exert direct or indirect modulatory effects on calcineurin/calmodulin/nuclear factor of activated T-cell pathways.[46–53] These findings imply that the calcineurin signaling pathway might play a central pathomechanistic role in PTC damage in patients with CINAC. On top of the highly reabsorptive capacity of the PTCs, renal calcineurin phosphatase activity is highest in these cells, likely accounting for the localization of the injury.[54] Importantly, several of the most widely used pesticides in Sri Lanka and El Salvador, including paraquat, glyphosate, and pyrethroids, have direct or indirect calcineurin inhibitory actions.[23–28] Additionally, patients with CINAC are prone to the development of infections, indicating some level of immunosuppression.[55] Furthermore, cyclosporine, tacrolimus, and some pesticides also inhibit sodium–potassium adenosine triphosphatase, possibly explaining electrolyte disturbances in these patients (Supplementary Table S2).[56,57] For the other toxic compounds such as African herbs (a complex mixture of many unknown herbs) and allopurinol, direct links to calcineurin are currently lacking or not investigated, thereby leaving the possibility for involvement of other pathways open. The overarching theme, however, is that exposure to toxic compounds is clearly associated with the occurrence of the aberrant lysosomal phenotype and that interference with different pathways may converge to the observed phenotype.

Although CINAC and cyclosporine/tacrolimus toxicity parallel in several physiologic/histopathologic aspects, they are unlikely to match in every disease aspect. Abstraction must be made between effects caused by calcineurin inhibition versus interference with other cellular processes/pathways. Although the effects of cyclosporine/tacrolimus on the renin–angiotensin system, endothelin, and other hemodynamic actors are well documented, currently no clear-cut proof exists that they are actually due to CNI.[39] Also, whereas cyclosporine inhibits the renin–angiotensin system, pesticides have not been reported to do so. Pesticide exposure is expected to be orders of magnitudes smaller compared with patients treated daily with cyclosporine/tacrolimus. Although speculative at this stage,

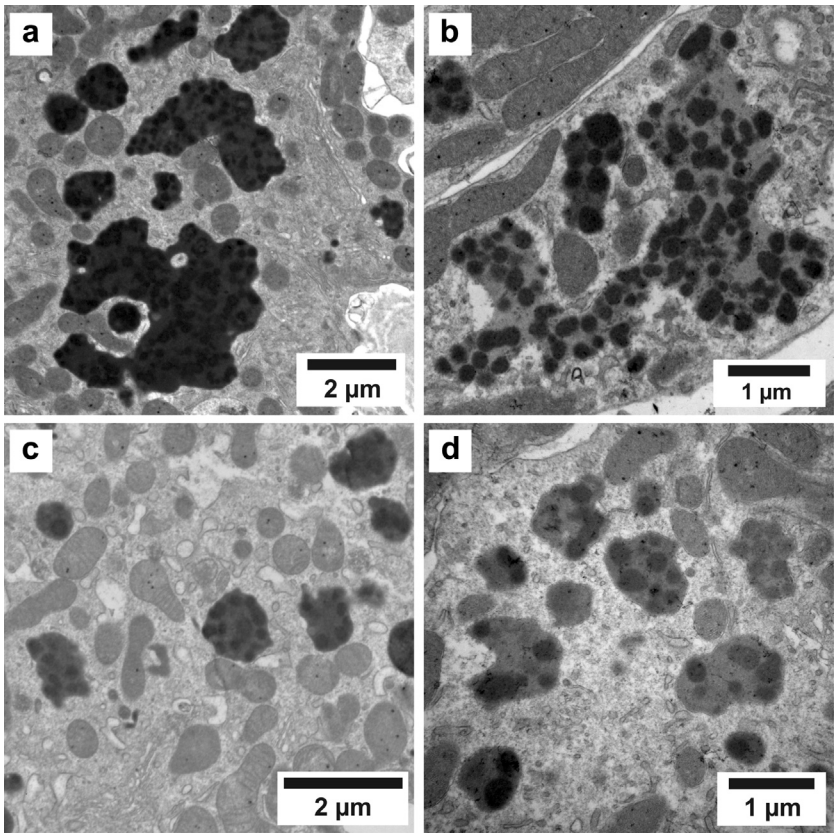

Figure 10 | Phenotypical variability of the lysosomal lesion. Two very large dysmorphic lysosomes are accompanied by several smaller ones (**a**). All contain dispersed electron-dense aggregates. An extremely dysmorphic lysosome containing aggregates against a slightly paler matrix (**b**). Examples of clusters of smaller dysmorphic lysosomes containing aggregates (**c,d**). Images are from Sri Lankan patients with Chronic Interstitial Nephritis in Agricultural Communities. To optimize viewing of this image, please see the online version of this article at www.kidney-international.org.

CINAC nonetheless may develop as the result of a potent calcineurin inhibitory action to which the inherently heavily exposed proximal tubule is extremely vulnerable.

Repeated episodes of severe dehydration have been proposed as a cause of CINAC.[58,59] However, recent reviews have pointed out the increasing worldwide incidence of CINAC in concert with agricultural mechanization in the 1990s, the absence of CINAC in hotter northern Sri Lanka and Cuba where agrochemicals are rarely or ever used, the mosaic geographic pattern of CINAC in endemic areas despite a uniform overall climate and type of agricultural activity, and the presence of CINAC among woman, children, and adolescents who are not exposed to harsh working conditions.[2,3,7] Thus there is epidemiological evidence that CINAC is not solely a dehydration-induced disease, and histopathological evidence is lacking.[2] However, increasing evidence shows that CINAC might be related to agrochemical exposure.[60–66] Insecticides and herbicides, some with suggested nephrotoxicity, have been applied extensively in sugar cane fields, paddy fields, and vineyards since the late 1980s.[67–70] A higher prevalence of CINAC is seen in people exposed to stationary drinking water from ground wells in contrast to serving wells in endemic regions, suggesting exposure to toxins through contaminated drinking water or other routes of (in)direct exposure.[62] Our morphologic findings add a strong argument to CINAC's toxic etiology. In

Table 1 | Diagnostic criteria of the aberrant lysosomal phenotype

	Observed phenotype	Diagnostic interpretation
Light microscopy	Presence of enlarged proximal tubular cell argyrophylic granules (identified as lysosomes) in association with varying degrees of epithelial simplification, tubular atrophy, luminal cell fragment shedding with or without tubulointerstitial expansion (inflammation, edema, fibrosis)	Suggestive (requiring electron microscopy confirmation!)
Electron microscopy	Presence of enlarged (>1.2 µm) dysmorphic lysosomes containing dispersed rounded/irregular electron dense aggregates	Confirmed
	Presence of 2 or more clusters of ≥3 lysosomes that meet the aforementioned criteria of intralysosomal aggregates and mild to moderate dysmorphia but are smaller than 1.2 µm in greatest diameter	Suspicious

Table 2 | Relevant clinical data and assessment of the lysosomal phenotype by electron microscopy of patients with CINAC

Patient no.		Sex	Age, yr	S-creatinine, mg/dl	Proteinuria[a]	Blood pressure, mm Hg	eGFR, MDRD	Heat exposure[b]	Lysosomal phenotype (EM confirmation)
Sri Lanka	1	M	47	1	Moderate	140/90	85	No	Yes
	2	M	37	1.8	Nil	100/70	46	No	Yes
	3	M	49	2	Trace	110/80	38	Yes	No
	4	F	34	2.1	Nil	140/90	29	No	Yes
	5	M	68	1.81	Trace	130/80	38	No	Yes
	6	M	59	3.09	Trace	150/80	21	Yes	Yes
	7	M	38	1.28	Trace	140/80	70	Yes	No
	8	F	30	4.56	Severe	150/80	12	No	Inadequate sample[c]
	9	M	61	1.65	Trace	130/80	44	No	Yes
	10	F	34	0.81	Severe	110/60	94	No	Yes
	11	F	28	2.34	Severe	130/80	27	No	Yes
	12	M	42	2.6	Trace	140/80	29	Yes	Yes
	13	M	45	2.28	Trace	130/80	33	No	Inadequate sample[c]
	14	M	60	1.5	Nil	110/70	51	Yes	Yes
	15	M	53	1.7	Nil	110/60	45	yes	No
	16	M	61	1.52	Trace	120/70	50	Yes	Yes
	17[d]	M	71	2.3	Nil	150/90	30	Yes	No
	18[d]	M	58	2.7	Severe	130/80	26	No	Yes
El Salvador	19	F	38	0.8	Trace	120/70	80	No	Yes
	20	M	53	2	Moderate	120/80	53	Yes	Yes
	21	M	54	1.3	Nil	130/70	58	Yes	Suspicious[e]
	22	F	41	0.8	Nil	120/80	79	No	Suspicious[e]
	23	M	50	1.4	Nil	130/80	54	No	Yes
	24	M	36	1.1	Nil	100/60	76	Yes	Yes
	25	M	59	1.4	Trace	120/80	59	Yes	Yes
	26	M	49	1.9	Nil	150/80	33	No	Yes
	27	M	34	1.4	Nil	100/60	58	No	Yes
	28	M	36	1	Nil	100/70	85	No	Yes
	29	M	31	1.3	Nil	110/70	68	NA	Yes
India	30	M	54	2.3	Moderate	130/85	32	No	Yes
France	31	F	73	5.7	Moderate	NA	30	No	Yes
	32	M	45	2.03	NA	90/70	6	No	Yes
	33	M	47	2.07	Trace	150/96	58	No	Yes
	34	F	72	1.9	Trace	NA	20	No	Yes

CINAC, Chronic Interstitial Nephritis in Agricultural Communities; eGFR, estimated glomerular filtration rate; EM, electron microscopy; F, female; M, male; MDRD, Modification of Diet in Renal Disease; NA, not available.

[a]Proteinuria: nil (negative on dipstick), trace < moderate (1–3.4 g/ml or <1500 mg/24 hr) < severe.

[b]Heat stress was defined as working under direct sun exposure during the day while working in the field in Sri Lanka. In El Salvador, heat stress was determined as working under conditions over 30 °C for more than 4 hours.

[c]Inadequate sample: medullary tissue, no proximal tubules, autolysis, no reprocessing possible.

[d]Patients with type 2 diabetes.

[e]Suspicious is defined by the presence of 2 or more clusters of ≥3 lysosomes that meet the criteria of aggregates and dysmorphia but are smaller than 1.2 μm in greatest diameter.

particular, EM analysis of implantation versus CNI-exposed protocol biopsy specimens unequivocally demonstrated the appearance of the aberrant lysosomes in association with CNI exposure, suggesting that CINAC is an acquired lysosomal tubulopathy. With respect to transplant biology itself, this investigation is the first to report an abberant lysosomal phenotype in patients treated with CNIs, which can occur in the absence of decreased renal function. It remains to be determined whether the presence of such lysosomal features is an early marker of toxicity, predicting graft survival.

In our cyclosporine-treated rats, the absence of glomerular lesions together with the early presence of a similar lysosomal lesion with focally associated tubular atrophy and early tubulointerstitial fibrosis indicate that PTCs are a primary target of CNI nephrotoxicity. Grgic *et al.*[71] elegantly demonstrated that repeated PT toxic injury leads to tubular injury, tubular atrophy, tubulointerstitial fibrosis, and secondary glomerulosclerosis. In a prospective histopathologic study of 11 Nicaraguan patients with MeN, biopsied at their earliest clinical appearance, Fischer *et al.*[72] reported a primary tubulointerstitial disease with largely preserved glomeruli. The dehydrated rats had slight glomerular shrinking but no tubulointerstitial fibrosis or increased number of enlarged dysmorphic lysosomes after 4 weeks. Our findings corroborate a 1963 study of Sabour *et al.*[73] who studied rat renal tissue by LM and EM after acute dehydration. LM showed no histologic abnormalities. On EM, PTCs appeared normal and lysosomes lacked dysmorphic features. Our findings, however, are in contrast to the work of Roncal Jimenez *et al.*,[59] who observed PT injury and mild

Table 3 | Healthy control subjects and non-CINAC nephropathies investigated for the aberrant lysosomal phenotype

Clinical condition	*n*	Lysosomal phenotype (EM-confirmed)	
Drug exposure and toxic nephropathies	**22**	Yes	Suspicious[a]
Tenofovir-treated HIVAN	7	1	0
Cisplatinum	4	0	0
Lithium	9	7	0
Lomustine	1	1	0
Clomiphene	1	1	0
Calcineurin inhibitor treatment	**27**		
Renal transplant indication biopsy	21	16	2
Nonrenal transplant kidney biopsy	6	6	0
Interstitial nephritis	**19**		
Acute, chronic, or mixed interstitial nephritis	15	4[b]	3
Pyelonephritis	4	0	2
Proteinuric nephropathies	**16**		
Light chain disease	5	2	0
Diabetes	5	0	0
Minimal change disease	3	0	0
Lupus	2	0	0
Tip variant focal segmental glomerulosclerosis	1	0	0
Non-CINAC Sri Lankan nephropathies	**6**		
Mixtures of focal segmental glomerulosclerosis, minimal change, glomerulonephritis, tubulointerstitial nephritis	6	1	1
Healthy control	**10**	1[c]	0

CINAC, Chronic Interstitial Nephritis in Agricultural Communities; EM, electron microscopy; HIVAN, HIV-associated nephropathy.
[a]Suspicious is defined by the presence of 2 or more clusters of ≥3 lysosomes that meet the criteria of aggregates and dysmorphia but are smaller than 1.2 μm in greatest diameter.
[b]Positive cases were drug induced: allopurinol ($n = 2$), cocaine ($n = 1$), African herbs ($n = 1$).
[c]Positive control case was from Sri Lanka.

tubulointerstitial fibrosis in mice after 5 weeks of a slightly more severe recurrent dehydration model compared with our study. Although the PTCs were injured, lysosomal abnormalities were not described. In our study, the notable PT lysosomal enlargement/accumulation/dysmorphia and tubular damage/atrophy observed in cyclosporine-treated rats and their absence in dehydrated rats makes the heat stress/dehydration hypothesis unlikely as the primary cause of CINAC. The fact that in our CINAC cohort only 7 of 26 patients (26%) with proven aberrant lysosomes presented heat exposure (Table 2) further corroborates the unlikelihood of this hypothesis. However, it cannot be excluded that, in limited cases of proven repetitive dehydration, this pathophysiological status may contribute to disease by its effect on particular molecular pathways or, alternatively, by increasing local renal toxicant concentrations.

With respect to the natural course of CINAC, the early-stage renal biopsy study of Fischer *et al.*[72] in Nicaraguan patients with MeN reported patchy tubular cell injury/atrophy and interstitial inflammation in the cortex and corticomedullary junction, without involvement of glomeruli, leading the authors to conclude that an infectious or toxic agent is a likely initial cause of renal injury. Targeted toxic injury to the PTCs is sufficient to trigger a primary inflammatory response.[71] Moderate or severe fibrosis and inflammation were observed in 35.3% and 29.4% of our human biopsies, respectively. This finding is consistent with initiation of a local inflammatory/fibrotic event by a primary toxic PT insult, with secondary atrophy and glomerulosclerosis.

PTCs of patients with CINAC exhibit minimal proliferation and no apparent apoptosis, suggesting that these cells are in a senescent state. The prominent distal tubular proliferation and apoptosis suggest distal compensation for the PT functional deficiency due to toxic injury.[74] The apparent loss of cytoplasmic fragments on the apical PTC aspect may contribute to cell injury/loss and ultimate tubular atrophy. The exact mechanisms by which PTCs are lost is yet unknown.

Our study has limitations. First, although we included a broad spectrum of control renal diseases, the number of patients is limited. Nonetheless, the vast majority of clinically diagnosed patients with CINAC showed PTC-enlarged lysosomes. Second, this study is qualitative. A systematic quantitative morphometric analysis of the described lesions in patients with CINAC, transplant patients treated with CNIs, and larger cohorts of pathologic and nonpathologic control subjects is the next step. Third, 18.7% of CINAC samples did not show the abberant lysosomes on EM, probably because of the inherent small EM sample size. Fourth, although we observed dysmorphic enlarged PTC lysosomes associated with varying degrees of tubular atrophy and cell fragment shedding in CINAC and CNI, we do not provide proof that the abnormal lysosomes are responsible for the PT atrophy and absence of regeneration. Fifth, the suggested involvement of the calcineurin pathway in patients with CINAC currently is not proven, although it is clearly suggested by the histopathologic parallels between the different nephropathies and data in the literature. We cannot exclude the possibility of other pathway involvement, nor do we explain how putative calcineurin inhibition may lead to a lysosomal tubulopathy. Sixth, although the protocol for visualizing lysosomes by Jones stain is optimized, the argyrophilic and fluorescent components in the lysosomes are currently unknown (Supplementary Methods). Seventh, our current report does not contain a toxicologic analysis. A toxicologic/metabolomic analysis by liquid chromatography high-resolution tandem mass spectrometry on endemic water samples and urine and renal tissue from patients with CINAC likely would identify the putative CINAC-inducing toxin(s).

Diagnostic performance

The finding of an increased number of large PTC dysmorphic lysosomes associated with varying degrees of epithelial atrophy and cell fragment shedding by LM (Jones staining and/or autofluorescence) in patients with no or low levels of proteinuria living in an agricultural environment is indicative of CINAC. However, confirmation by

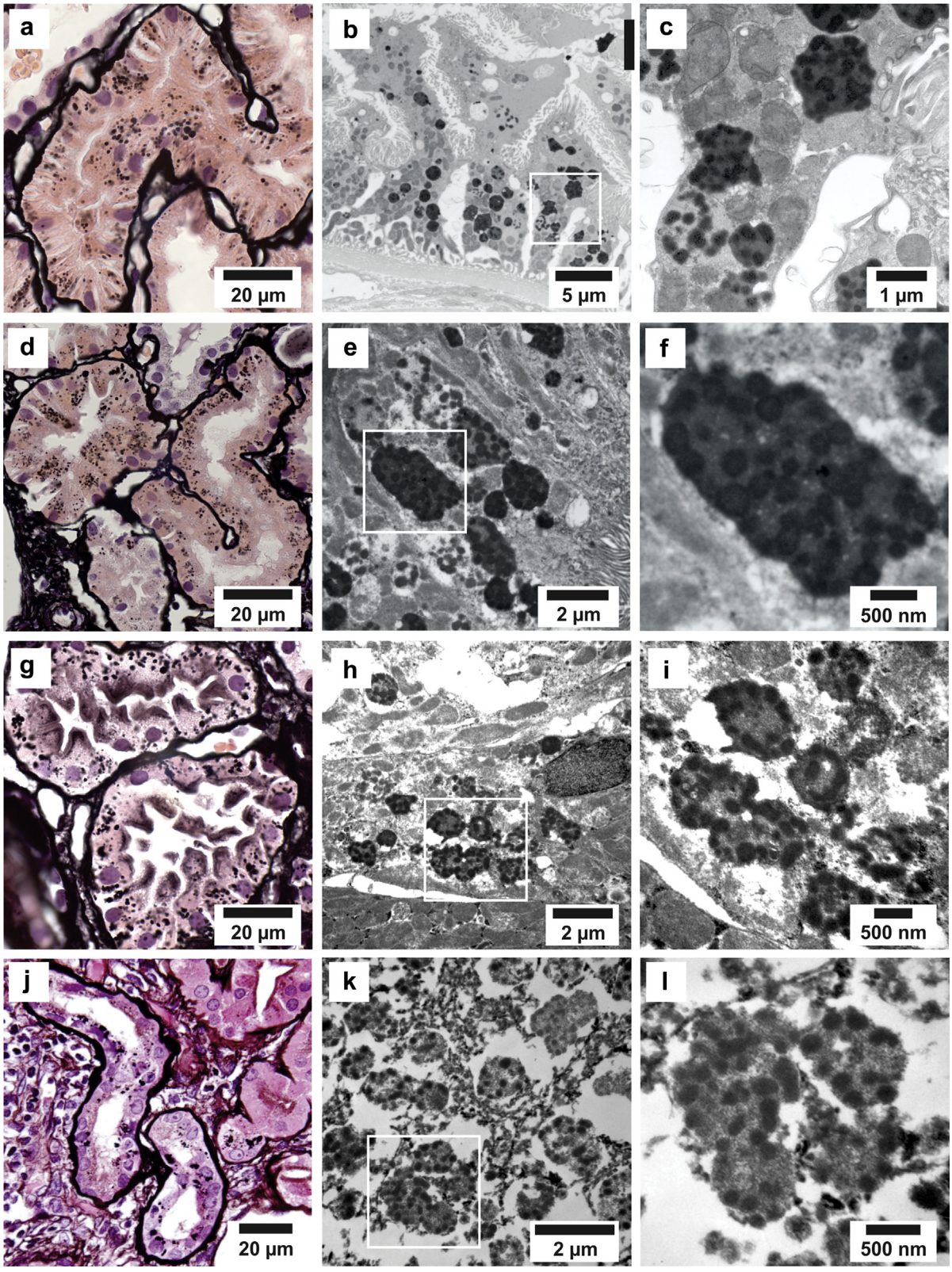

Figure 11 | The aberrant lysosomal phenotype is consistent throughout patients with Chronic Interstitial Nephritis in Agricultural Communities from different regions. Sri Lanka (**a–c**), El Salvador (**d–f**), India (**g–i**), and France (**j–l**). To optimize viewing of this image, please see the online version of this article at www.kidney-international.org.

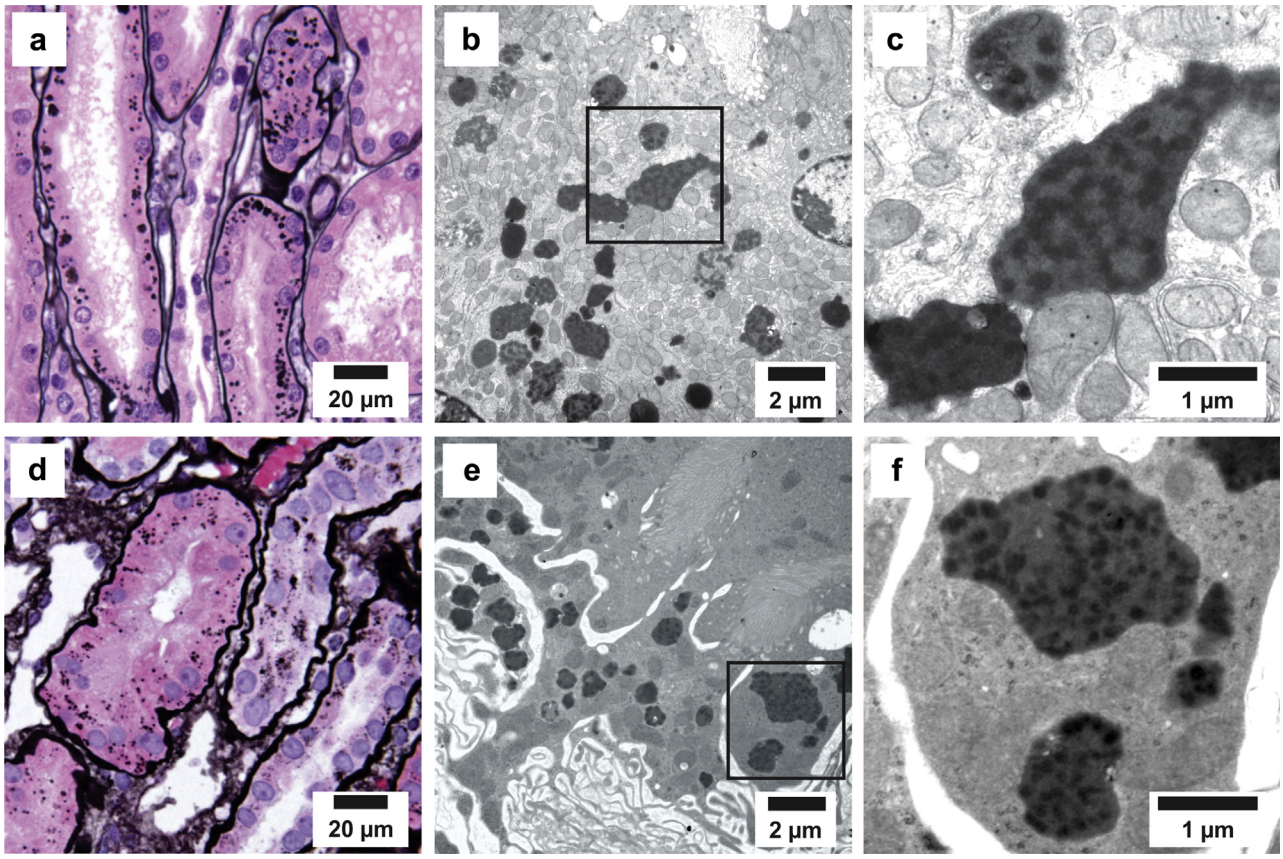

Figure 12 | Enlarged dysmorphic lysosomes in transplant patients undergoing immunosuppressive therapy with calcineurin inhibitors. Cyclosporine (**a–c**). Tacrolimus (**d–f**). See also Supplementary Figure S12. To optimize viewing of this image, please see the online version of this article at www.kidney-international.org.

EM substantially increases the diagnostic sensitivity because it unequivocally identifies the large PTC dysmorphic lysosomes containing dispersed dark rounded aggregates (Table 1). In some control subjects and proteinuric patients, increased numbers and sizes of PTC argyrophilic lysosomes can be seen by LM, thus requiring EM analysis to identify CINAC lysosomes. CINAC and type 2 diabetes can coexist, thereby demonstrating that diabetes can no longer

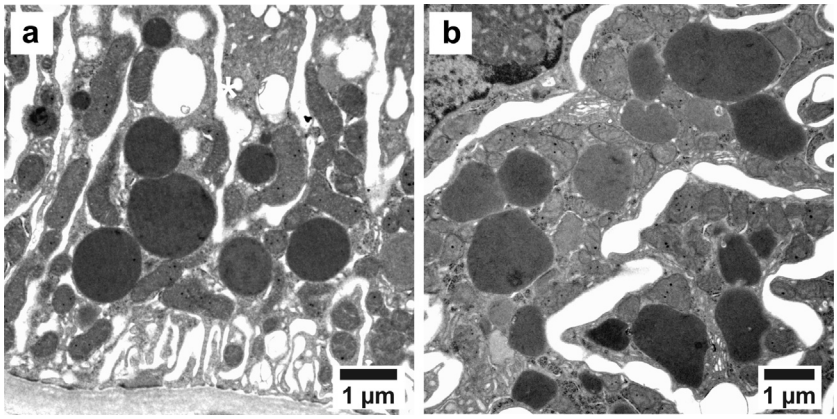

Figure 13 | Lysosomal phenotypes in patients with overt proteinuria. Lysosomes can be enlarged with a round to slightly irregular shape. Their contents are homogenous, rarely with some scattered membranous structures or peripheral electron-dense aggregates, but consistently without the numerous dispersed dark electron-dense aggregates found in the Chronic Interstitial Nephritis in Agricultural Communities patient lysosomes. (**a**) Lysosomes of a patient with minimal change disease and a serum creatinine level of 1.3 mg/dl. (**b**) Lysosomes of a patient with tip lesion focal segmental sclerosis and a serum creatinine level of 0.83 mg/dl. To optimize viewing of this image, please see the online version of this article at www.kidney-international.org.

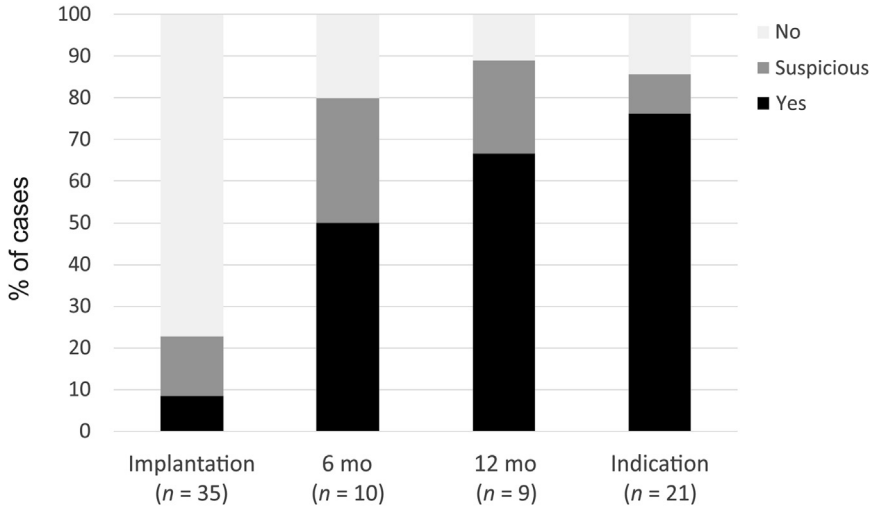

Figure 14 | Bar graph presenting the percentage of cases positive for the aberrant lysosomal phenotype for each condition. The lysosomal phenotype is clearly acquired in association with calcineurin inhibitor exposure. Suspicious cases are defined by the presence of clusters of 3 to 5 lysosomes that meet the criteria of aggregates and dysmorphity but are smaller than 1.2 μm.

be considered an absolute exclusion criterion in the clinical diagnosis of CINAC.

Conclusions

PTC lysosomal lesions (suggested by Jones staining and LM and confirmed by EM) associated with varying degrees of epithelial atrophy and cell fragment shedding were found in 81.3% of renal biopsy specimens from patients with CINAC in Sri Lanka, El Salvador, India, and France who were diagnosed according to current clinical criteria.[2] The identical clinical and pathologic phenotype of CINAC in different locations supports involvement of common pathophysiological pathways. The majority of patients treated with CNIs acquire similar lesions in their PTCs, which contain abundant calcineurin. The documented CNI effect of some herbicides and insecticides (e.g., paraquat, glyphosate, and pyrethroids) suggests a pathway leading to the striking similarity of PT lesions in these 2 forms of toxic nephropathy.[23–28] Overall these findings strongly suggest a toxicologic etiology for the global presence of CINAC.

METHODS

Patient material

CINAC/MeN/CKDu renal biopsy samples were included when patients met 4 of 5 of the following clinico-epidemiologic criteria[2,8]: patients with CKD living in agricultural environment, living in a CINAC-endemic region, no trace proteinuria, no diabetes, and no high blood pressure (Table 2). Two patients with type 2 diabetes and clinically confirmed CINAC were included. Healthy control renal biopsy specimens were from transplant kidneys at implantation (n = 35), uninvolved renal parenchyma from tumor nephrectomies (n = 6), and necropsy tissue (n = 4) (Table 3 and Figure 14). Pathologic control renal biopsy specimens were from proteinuric nephropathies, non-CINAC glomerulopathies, toxic nephropathies, and patients taking CNIs (among which 6-month [n = 10] and 12-month [n = 9] renal transplant protocol biopsies and indication biopsies [n = 21] were included) (Table 3 and Figure 14). Of the 35 renal transplant patients whose implantation biopsies were analyzed, 10 had an additional biopsy specimen available at 6 and 12 months, respectively. At 12 months, one sample preparation did not allow proper analysis, hence the number was 9. Biopsy samples were made available via many collaborators (see Acknowledgments).

Rat study

Eight-week-old male Wistar rats (Charles River, France) were divided in 3 groups. Group 1 ($n = 6$) had water ad libitum (control group). Group 2 ($n = 8$) was water deprived for 10 hours per 24 hours, 5 days per week. During water deprivation, rats were placed in an incubator (37 °C) for 30 minutes each hour. Group 3 ($n = 8$) was administered 50 mg/kg body weight of cyclosporine (Neoral-Sandimmune, Novartis, Basel, Switzerland) by daily oral gavage. Study duration was 4 weeks. Study details are available in Supplementary Methods. All experimental procedures were conducted according the National Institutes of Health Guide for the Care and Use of Laboratory Animals and approved by the Ethical Committee of the University of Antwerp.

Histological analysis

Kidney tissue was fixed in paraformaldehyde, formalin, or alcoholic Bouin's fixative, embedded in paraffin, and cut into 2- to 4-μm-thick sections. LM analysis was performed using periodic acid–Schiff and, predominantly, Jones silver methenamine–stained renal cortical tissue sections counterstained with hematoxylin and eosin. Jones silver stain was performed according to adapted procedures (Supplementary Methods and Supplementary Figure S15). Lysosomal acid phosphatase enzymatic activity was performed on frozen sections (6 μm) following the Lojda method as reported previously.[33] For immunofluorescent analysis, tissue sections were labeled with primary antibody and corresponding Alexa Fluor conjugated secondary antibodies (Thermo Fisher Scientific, Rockford, IL). For immunohistochemistry, biotinylated secondary antibodies (Vector Laboratories, Burlingame, CA) were used for avidin-biotin-peroxidase mediated staining. Primary antibody details are provided in Supplementary Methods (Supplementary References).

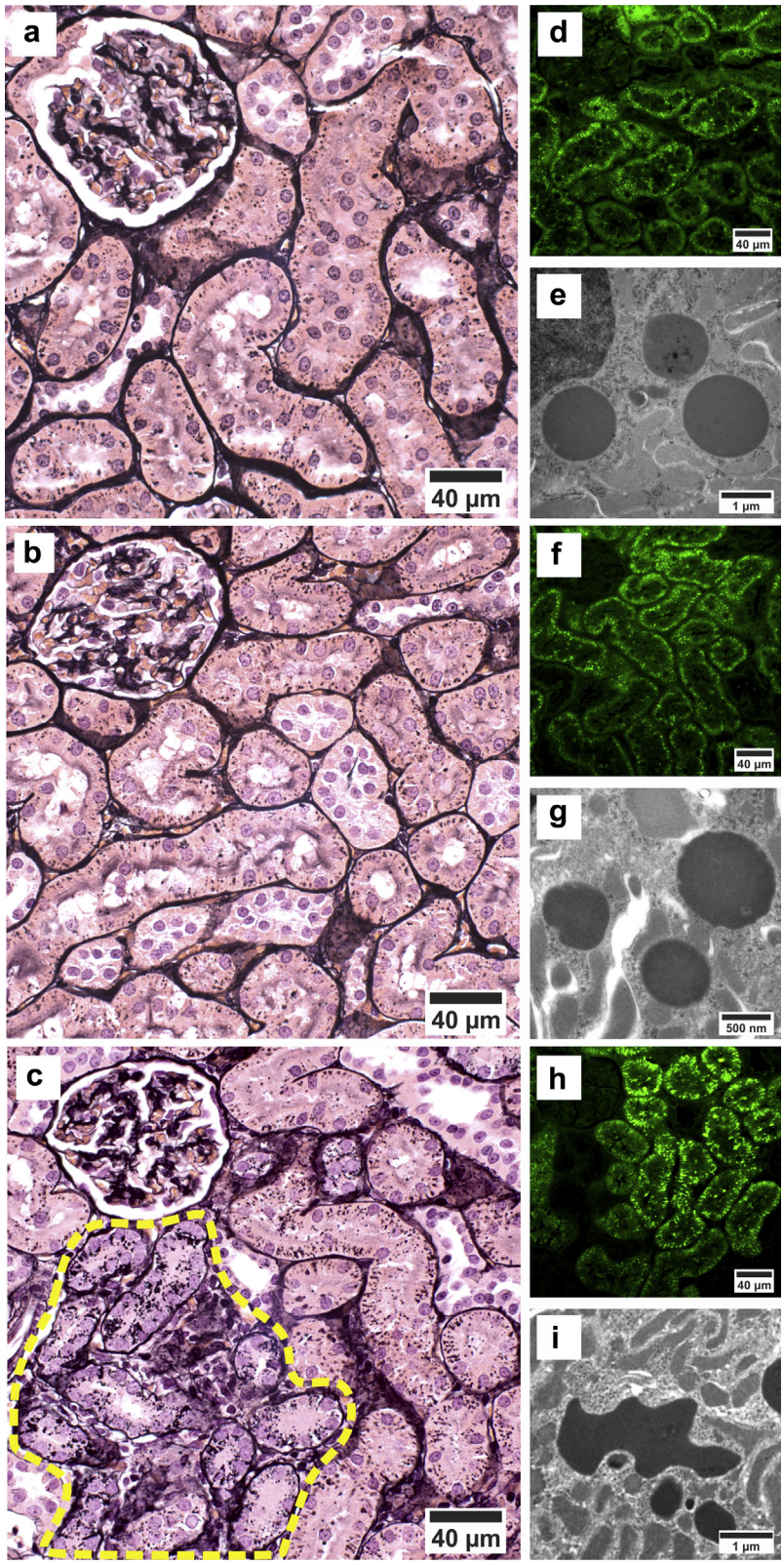

Figure 15 | Renal histopathology in rats undergoing chronic dehydration (b,f,g) or cyclosporine treatment (c,h,i) compared with control subjects (a,d,e). Control and dehydrated animals had similar scattered proximal tubule granules with positive Jones staining (**a,b**), weak to moderate autofluorescence (**d,f**), and a rounded fairly uniform appearance by electron microscopy (**e,g**), respectively. Cyclosporine-treated rats demonstrated an increased lysosomal number, size, and intensity both on Jones stain (**c**) and autofluorescence (**h**). In addition, a subset of lysosomes demonstrated a dysmorphic appearance (**i**) that was not observed in the other groups. Jones stain also revealed foci of early atrophy in tubules with prominent lysosomes in cyclosporine-treated rats (**c**, yellow dotted line) but not in the other groups. To optimize viewing of this image, please see the online version of this article at www.kidney-international.org.

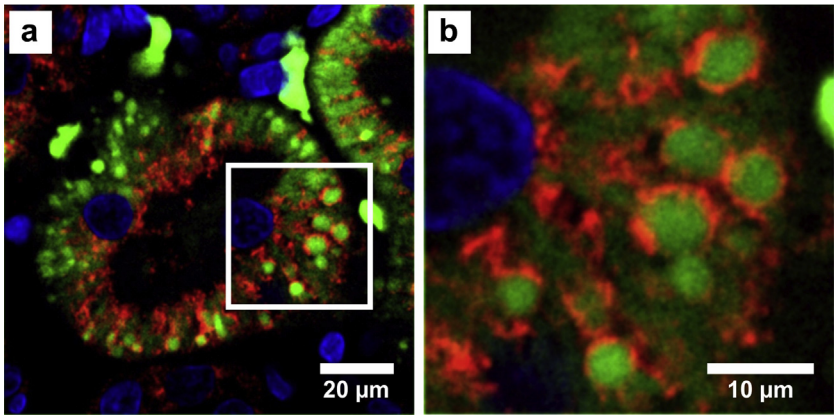

Figure 16 | Tubular cell lysosomes in rats treated with cyclosporine. As in human patients with Chronic Interstitial Nephritis in Agricultural Communities, staining with lysosomal-associated membrane protein 1 (red) delineates enlarged green autofluorescent lysosomes (green). A higher magnification of (**a**) is shown in (**b**). Nuclear counterstain was performed with Hoechst33342. To optimize viewing of this image, please see the online version of this article at www.kidney-international.org.

Autofluorescence

Autofluorescent characteristics were analyzed on 4-µm tissue sections after a standard deparaffination procedure with toluene (Fisher Scientific, Loughborough, UK). To maintain autofluorescent contrast, high purity solvents without contamination (e.g., water) are required. For imaging (performed with a Leica DMRB microscope [Buffalo Grove, IL] with a Zeiss AxioCam HRc camera [Jena, Germany]), a shutter time between 2 and 7 seconds at 400× was used. Image processing and analysis was performed with Fiji open source software.[75]

EM

Samples fixed in glutaraldehyde were postfixed in OsO_4 and embedded in epoxy resin. Reprocessing of formalin-fixed paraffin-embedded samples involved deparaffinization, rehydration, and embedding in epoxy resin. Ultrathin sections were collected on carbon-coated formvar grids and stained with uranyl acetate and lead. Electron microscopes were Tecnai G2 Spirit Bio Twin (FEI, Eindhoven, The Netherlands), JEOL 100 CX (JEOL, Peabody, MA), and Hitachi 7700 (Hitachi, Santa Clara, CA). The chemical compositions on grids prepared from Jones-stained tissue slides were obtained by energy dispersive x-ray spectroscopy using a Tecnai Osiris (FEI, Hillsboro, OR) transmission electron microscope operating at 200 kV and equipped with Super-X detector.

Statistics

Data are given as mean ± SD. Statistical analysis was performed using Kruskal-Wallis and Mann-Whitney U tests through use of Graphpad Prism (GraphPad Software, San Diego, CA). P values <0.05 were considered statistically significant.

DISCLOSURE

All the authors declared no competing interests.

ACKNOWLEDGMENTS

The following people and laboratories contributed by providing biopsy specimens and technical support for confocal and electron microscopic imaging and histological and biochemical analysis: S. Dauwe, I. Pintelon, D. De Weerdt, A. Dendooven, J.L. Bosmans, L. Djukanovic, L. Janković-Veličković, A. Vital, M. Depierreux, J. Nortier, C. Jounneau, S. Gunatilake, M. Funes de la Vega, R. Herrera, L. Lopez, M. Almaguer, V. Gnemmi, A. Lionet, T. Sqalli Houssaini, I. Brocheriou, E. Rondbatt, A. Mokteri, A. Ferreira, M. Góis, S. Siribaddana, M. Berghmans, L. Pieters, A. Nuyts, F. Glowacki, G. Gobe, J.T. Deng, P. Delputte, P. Rieu, C. Combe, N. Noel, B. Chauveau, A. Servais, R.R. Tatapudi, Labo Lokeren BVBA, clinical biology laboratory of Antwerp University Hospital, Laboratory of Pathological Anatomy AZ St-Niklaas (I. De Gendt, S. De Prez), Histology lab Ugent (L. Pieters), Faculty of Medicine VUB (M. Berghmans), Laboratory of Pathology UZGent (M. Praet, J. Van Dorpe), EMAT UAntwerp (D. Schrijvers), and EM Laboratory of Cedars-Sinai (W. Lungo, D. Leal). Lions Club Lokeren took care of travel costs of CJ in 2017. This project received funding in part from Research Foundation Flanders (PhD Fellowship Gerd Schreurs 1S52218N and Research Grant G0C0119N).

SUPPLEMENTARY MATERIAL

Supplementary Methods. Secondary antibody details for immunohistochemistry/fluorescence, study details of the rat study (cyclosporine vs. dehydration), and protocol methenamine silver staining (Jones staining) and comments.

Supplementary Data. Body weight and serum/urine biochemistry of the rat study.

Table S1. Kidney biopsy light microscopic findings in patients with CINAC from Table 2.

Table S2. Parallels between patients with CINAC and cyclosporine/tacrolimus-treated transplant patients.

Figure S1. Examples of some nonspecific lesions that can be observed in CINAC biopsy specimens: tubulointerstitial fibrosis, mild inflammatory infiltration, thickening of basement membranes, and tubular atrophy (**A**) and isometric vacuolization (black arrows; **B**). Renal tissue from the Sri Lankan CINAC cohort.

Figure S2. Overview and details of an adapted version of the Jones protocol without gold chloride step and counterstain. Granules (i.e., lysosomes) appear in shades of brown, allowing discernment of a dysmorphic nature (**A,B**), as well as, for the bigger ones, an internal darker clumped material (**C,D**). Images from an Indian patient with CINAC.

Figure S3. Tubules with accumulation of granules are of proximal tubular nature. Granules can be identified by their argyrophylic properties (Jones staining), as well as by their autofluorescence on unstained sections (see Supplementary Figure S5). (**A**) Autofluoresence on section stained for the S3 proximal segment marker intestinal alkaline phosphatase (IAP) seen in **B**. (**C**) Autofluoresence on section serial to a section stained with leucine

aminopeptidase (LAP) seen in **D**. Both the IAP and LAP staining demonstrate intracellular granules positive for these respective markers, indicative of lysosomes (black arrows). Renal tissue from the Sri Lankan CINAC cohort.

Figure S4. Cell blebbing and cell fragment shedding of granule-containing proximal tubular epithelia observed on Jones stained tissue sections. Apparent apical blebbing (solid arrows; **A**). Focally, tubules can present cell fragments, with and without Jones positive granules, that appear to have shed into the lumen (open arrows; **B**). Renal tissue from the Sri Lankan CINAC cohort.

Figure S5. The mitochondrial marker COX6C (red) is not or scarcely expressed in tubules with autofluorescent vesicles (green; **A,B**). Blue: nuclear counterstain with Hoechst33342. Renal tissue from the Sri Lankan CINAC cohort.

Figure S6. Additional confocal images of immunofluorescent staining for the lysosomal markers cathepsin B (**A**) and LAMP1 (**B**). Red: lysosomal marker; green: autofluorescence; blue: nuclear counterstain with Hoechst33342; yellow/orange: merging of lysosomal markers with autofluorescence. Renal tissue from the Sri Lankan CINAC cohort.

Figure S7. Autofluorescent image of CINAC biopsy specimen (**A**). Serial section to **A** stained for enzymatic activity of the lysosomal enzyme acid phosphatase showing granular positivity in affected tubules (**B**). Serial section to **A** stained for the proximal tubular marker leucine aminopeptidase (LAP; **C**). Renal tissue from the Sri Lankan CINAC cohort.

Figure S8. Sequential magnifications (**A–C**) show that the lysosomes are single-membrane bound and that the intralysosomal dark aggregates are nonmembrane bound and lack a substructure. Images from Sri Lankan CINAC cohort.

Figure S9. Bar graph of size-frequency distribution of the 140 largest lysosomes selected from EM images across the Sri Lankan CINAC cohort ($n = 12$).

Figure S10. Arrows point toward swollen, degenerating mitochondria, which are not to be mistaken for the typical CINAC/CNI lysosomes. Renal tissue of a non-CINAC patient from Sri Lanka.

Figure S11. The aberrant lysosomal phenotype is observed in several toxin-induced nephropathies. Light chain disease (**A–C**), lomustine (**D–F**), clomiphene (**G–I**), and lithium (**J–L**) exposure. Jones staining in **A, D, G,** and **J**; EM in the other panels.

Figure S12. Additional examples of enlarged, dysmorphic lysosomes containing electron dense aggregates in transplant patients on cyclosporine (**A,B**) and tacrolimus (**C,D**) therapy.

Figure S13. Low and high magnification images of autofluorescence in rat renal tissue sections from control (**A,D**), dehydrated (**B,E**) and cyclosporine-treated (**C,F**) groups. Whereas **A, B, D,** and **E** show comparable autofluorescent granules, the cyclosporine-treated group (**C,F**) demonstrate increased granular size and brighter autofluorescence. Images were digitally edited (contrast, brightness) to optimally visualize separate autofluorescent granules.

Figure S14. High-magnification images of Jones stained rat renal tissue sections from control (**A**), dehydrated (**B**), and cyclosporine-treated (**C**) groups. Cyclosporine-treated rats show increased size and number of argyrophylic granules compared with control and dehydrated animals.

Figure S15. Variability of Jones staining on serial tissue sections. No to faint granular pattern within the proximal tubular epithelium (**A**). Jones staining with optimized (full-length) protocol reveals prominent accumulation of Jones positive granules (**B**). Biopsy specimen from a patient with CINAC from El Salvador.

Supplementary References.

Supplementary material is linked to the online version of the paper at www.kidney-international.org.

REFERENCES

1. Weaver VM, Fadrowski JJ, Jaar BG. Global dimensions of chronic kidney disease of unknown etiology (CKDu): a modern era environmental and/or occupational nephropathy? *BMC Nephrol*. 2015;16:2–8.
2. Jayasumana C, Orantes C, Herrera R, et al. Chronic interstitial nephritis in agricultural communities: a worldwide epidemic with social, occupational and environmental determinants. *Nephrol Dial Transplant*. 2017;32:234–241.
3. Ordunez P, Nieto FJ, Martinez R, et al. Chronic kidney disease mortality trends in selected Central America countries, 1997–2013: clues to an epidemic of chronic interstitial nephritis of agricultural communities. *J Epidemiol Community Health*. 2018;72:280–286.
4. Caplin B, Jakobsson K, Glaser J, et al. International collaboration for the epidemiology of eGFR in low and middle income populations—rationale and core protocol for the Disadvantaged Populations eGFR Epidemiology Study (DEGREE). *BMC Nephrol*. 2017;18:1.
5. Athuraliya N, Abeysekera T, Amerasinghe P, et al. Uncertain etiologies of proteinuric-chronic kidney disaese in rural Sri Lanka. *Kidney Int*. 2011;80:1212–1221.
6. Wijkström J, Jayasumana C, Dassanayake R, et al. Morphological and clinical findings in Sri Lankan patients with chronic kidney disease of unknown cause (CKDu): similarities and differences with Mesoamerican nephropathy. *PLoS One*. 2018;13:e0193056.
7. Herath C, Jayasumana C, Mangala P, et al. Kidney diseases in agricultural communities: a case against heat-stress nephropathy. *Kidney Int Rep*. 2018;3:271–280.
8. Wijkström J, Leiva R, Elinder C-G, et al. Clinical and pathological characterization of Mesoamerican nephropathy: a new kidney disease in Central America. *Am J Kidney Dis*. 2013;62:908–918.
9. López-Marín L, Chávez Y, García XA, et al. Histopathology of chronic kidney disease of unknown etiology in Salvadoran agricultural communities. *MEDICC Rev*. 2014;16:49–54.
10. Nayak A, Raikar A, Kotrashetti V, et al. Histochemical detection and comparison of apoptotic cells in the gingival epithelium using hematoxylin and eosin and methyl green-pyronin: a pilot study. *J Indian Soc Periodontol*. 2016;20:294–298.
11. Singh NP. A simple method for accurate estimation of apoptotic cells. *Exp Cell Res*. 2000;256:328–337.
12. Eskelinen EL, Kovács AL. Double membranes vs. lipid bilayers, and their significance for correct identification of macroautophagic structures. *Autophagy*. 2011;7:931–932.
13. Eskelinen E-L, Reggiori F, Baba M, et al. The impact of electron microscopy on autophagy research. *Autophagy*. 2011;79:935–956.
14. Eskelinen E-L. To be or not to be? Examples of incorrect identification of autophagic compartments in conventional transmission electron microscopy of mammalian cells. *Autophagy*. 2008;4:257–260.
15. Frank AL, Christensen AK. Localization of acid phosphatase in lipofuscin granules and possible autophagic vacuoles in interstitial cells of the guinea pig testis. *J Cell Biol*. 1968;36:1–13.
16. Perše M, Injac R, Erman A. Oxidative status and lipofuscin accumulation in urothelial cells of bladder in aging mice. *PLoS One*. 2013;8:e59638.
17. Appelqvist H, Wäster P, Kågedal K, et al. The lysosome: from waste bag to potential therapeutic target. *J Mol Cell Biol*. 2013;5:214–226.
18. Bandyopadhyay D, Cyphersmith A, Zapata JA, et al. Lysosome transport as a function of lysosome diameter. *PLoS One*. 2014;9:e86847.
19. De Broe ME, Giuliano RA, Verpooten GA. Choice of drug and dosage regimen. Two important risk factors for aminoglycoside nephrotoxicity. *Am J Med*. 1986;80:115–118.
20. Costa RM, Martul EV, Reboredo JM, et al. Curvilinear bodies in hydroxychloroquine-induced renal phospholipidosis resembling Fabry disease. *Clin Kidney J*. 2013;6:533–536.
21. Tulkens PM. Nephrotoxicity of aminoglycoside antibiotics. *Toxicol Lett*. 1989;46:107–123.
22. De Broe ME, Paulus GJ, Verpooten GA, et al. Early effects of gentamicin, tobramycin, and amikacin on the human kidney. *Kidney Int*. 1984;25:643–652.
23. Enan E, Matsumura F. Specific inhibition of calcineurin by type II synthetic pyrethroid insecticides. *Biochem Pharmacol*. 1992;43:1777–1784.
24. Jabłońska-Trypuć A, Wołejko E, Wydro U, et al. The impact of pesticides on oxidative stress level in human organism and their activity as an endocrine disruptor. *J Environ Sci Heal Part B*. 2017;52:483–494.
25. Ghosh MC, Wang X, Li S, et al. Regulation of calcineurin by oxidative stress. *Methods Enzymol*. 2003;366:289–304.

26. Lúcia de Liz Oliveira Cavalli V, Cattani D, Elise Heinz Rieg C, et al. Roundup disrupts male reproductive functions by triggering calcium-mediated cell death in rat testis and Sertoli cells. *Free Radic Biol Med*. 2013;65:335–346.
27. Webster TMU, Santos EM, Uren Webster TM, et al. Global transcriptomic profiling demonstrates induction of oxidative stress and of compensatory cellular stress responses in brown trout exposed to glyphosate and Roundup. *BMC Genomics*. 2015;16:32.
28. Wang X, Luo F, Zhao H. Paraquat-induced reactive oxygen species inhibit neutrophil apoptosis via a p38 MAPK/NF-κB-IL-6/TNF-α positive-feedback circuit. *PLoS One*. 2014;9:e93837.
29. Blair JT, Thomson AW, Whiting PH, et al. Toxicity of the immune suppressant cyclosporin A in the rat. *J Pathol*. 1982;138:163–178.
30. Kim JY, Suh KS. Light microscopic and electron microscopic features of cyclosporine nephrotoxicity in rats. *J Korean Med Sci*. 1995;10:352–359.
31. Duymelinck C, Dauwe SEH, Nouwen EJ, et al. Cholesterol feeding accentuates the cyclosporine-induced elevation of renal plasminogen activator inhibitor type 1. *Kidney Int*. 1997;51:1818–1830.
32. Mihatsch MJ, Thiel G, Basler V, et al. Morphological patterns in cyclosporine-treated renal transplant recipients. *Transplant Proc*. 1985;17:101–116.
33. Verpooten GA, Wybo I, Pattyn VM, et al. Cyclosporine nephrotoxicity: comparative cytochemical study of rat kidney and human allograft biopsies. *Clin Nephrol*. 1986;25(suppl 1):S18–S22.
34. Coen H, Roels F, Cornelis A, et al. Automated measurement of kidney lysosomes by light microscopy. Influence of cyclosporine treatment. *Anal Quant Cytol Histol*. 1988;10:87–93.
35. Herrera G. Renal diseases associated with hematopoietic disorders or organized deposits. In: Zhou XJ, Laszik ZG, Nadasdy T, et al., eds. *Silva's Diagnostic Renal Pathology*. Cambridge: Cambridge University Press; 2017:21–22.
36. Stokes MB, Valeri AM, Herlitz L, et al. Light chain proximal tubulopathy: clinical and pathologic characteristics in the modern treatment era. *J Am Soc Nephrol*. 2016;27:1555–1565.
37. Liu J. KF506 and cyclosporin, molecular probes for studying intracellular signal transduction. *Immunol Today*. 1993;14:290–295.
38. Sieber M, Baumgrass R. Novel inhibitors of the calcineurin/NFATc hub—alternatives to CsA and FK506? *Cell Commun Signal*. 2009;7:25.
39. Naesens M, Kuypers DRJ, Sarwal M. Calcineurin inhibitor nephrotoxicity. *Clin J Am Soc Nephrol*. 2009;4:481–508.
40. Sigal NH, Dumont F, Durette P, et al. Is cyclophilin involved in the immunosuppressive and nephrotoxic mechanism of action of cyclosporin A? *J Exp Med*. 1991;173:619–628.
41. Barton CH, Vaziri ND, Martin DC, et al. Hypomagnesemia and renal magnesium wasting in renal transplant recipients receiving cyclosporine. *Am J Med*. 1987;83:693–699.
42. Navaneethan SD, Sankarasubbaiyan S, Gross MD, et al. Tacrolimus-associated hypomagnesemia in renal transplant recipients. *Transplant Proc*. 2006;38:1320–1322.
43. Herrera R, Orantes CM, Almaguer M, et al. Clinical characteristics of chronic kidney disease of nontraditional causes in Salvadoran farming communities. *MEDICC Rev*. 2014;16:39–48.
44. Lee CH, Kim G-H. Electrolyte and acid-base disturbances induced by clacineurin inhibitors. *Electrolyte Blood Press*. 2007;5:126–130.
45. Bolzoni M, Donofrio G, Storti P, et al. Myeloma cells inhibit non-canonical wnt co-receptor ror2 expression in human bone marrow osteoprogenitor cells: effect of wnt5a/ror2 pathway activation on the osteogenic differentiation impairment induced by myeloma cells. *Leukemia*. 2013;27:451–463.
46. Mann DM, Vanaman TC. Modification of calmodulin on Lys-75 by carbamoylating nitrosoureas. *J Biol Chem*. 1988;263:11284–11290.
47. Harrison SD Jr, Mann DM, Giles RC Jr. Effect of nitrosoureas on calmodulin activity in vitro and in mouse intestine in vivo. *Cancer Chemother Pharmacol*. 1985;14:146–149.
48. Musgrove EA, Wakeling AE, Sutherland RL. Points of action of estrogen antagonists and a calmodulin antagonist within the MCF-7 human breast cancer cell cycle. *Cancer Res*. 1989;49:2398–2404.
49. Sutherland RL, Watts CK, Hall RE, et al. Mechanisms of growth inhibition by nonsteroidal antioestrogens in human breast cancer cells. *J Steroid Biochem*. 1987;27:891–897.
50. Davis J, Desmond M, Berk M. Lithium and nephrotoxicity: unravelling the complex pathophysiological threads of the lightest metal. *Nephrology*. 2018;23:897–903.
51. Gómez-Sintes R, Lucas JJ. NFAT/Fas signaling mediates the neuronal apoptosis and motor side effects of GSK-3 inhibition in a mouse model of lithium therapy. *J Clin Invest*. 2010;120:2432–2445.
52. Hu X-T, Ford K, White FJ. Repeated cocaine administration decreases calcineurin (PP2B) but enhances DARPP-32 modulation of sodium currents in rat nucleus accumbens neurons. *Neuropsychopharmacology*. 2005;30:916–926.
53. Addy NA, Bahi A, Taylor JR, et al. Administration of the calcineurin inhibitor cyclosporine modulates cocaine-induced locomotor activity in rats. *Psychopharmacology (Berl)*. 2008;200:129–139.
54. Tumlin JA. Expression and function of calcineurin in the mammalian nephron: physiological roles, receptor signaling, and ion transport. *Am J Kidney Dis*. 1997;30:884–895.
55. Gamage CD, Yoshimatsu K, Sarathkumara YD, et al. Serological evidence of hantavirus infection in Girandurukotte, an area endemic for chronic kidney disease of unknown aetiology (CKDu) in Sri Lanka. *Int J Infect Dis*. 2017;57:77–78.
56. Lea JP, Sands JM, McMahon SJ, et al. Evidence that the inhibition of Na+/K+-ATPase activity by FK506 involves calcineurin. *Kidney Int*. 1994;46:647–652.
57. Akera T, Brody TM, Leeling N. Insecticide inhibition of Na-K-ATPase activity. *Biochem Pharmacol*. 1971;20:471–473.
58. Glaser J, Lemery J, Rajagopalan B, et al. Climate change and the emergent epidemic of CKD from heat stress in rural communities: the case for heat stress nephropathy. *Clin J Am Soc Nephrol*. 2016;11:1472–1483.
59. Roncal Jimenez CA, Ishimoto T, Lanaspa MA, et al. Fructokinase activity mediates dehydration-induced renal injury. *Kidney Int*. 2014;86:294–302.
60. Orantes-Navarro CM, Herrera-Valdés R, Almaguer-Lopez M, et al. Chronic kidney disease in children and adolescents in Salvadoran farming communities: NefroSalva Pediatric Study (2009–2011). *MEDDIC Rev*. 2016;18:15–22.
61. Orantes-Navarro CM, Herrera-Valdés R, López MA, et al. Epidemiological characteristics of chronic kidney disease of non-traditional causes in women of agricultural communities of El Salvador. *Clin Nephrol*. 2015;83:24–31.
62. Jayasumana C, Paranagama P, Agampodi S, et al. Drinking well water and occupational exposure to herbicides is associated with chronic kidney disease in Padavi-Sripura, Sri Lanka. *Environ Health*. 2015;14:6.
63. Lebov JF, Engel LS, Richardson D, et al. Pesticide exposure and end-stage renal disease risk among wives of pesticide applicators in the Agricultural Health Study. *Environ Res*. 2015;143:198–210.
64. Lebov JF, Engel LS, Richardson D, et al. Pesticide use and risk of end-stage renal disease among licensed pesticide applicators in the Agricultural Health Study. *Occup Environ Med*. 2016;73:3–12.
65. Johnson RJ, Wesseling C, Newman LS. Chronic kidney disease of unknown cause in agricultural communities. *N Engl J Med*. 2019;380:1843–1852.
66. Chapman E, Haby MM, Illanes E, et al. Risk factors for chronic kidney disease of non-traditional causes: a systematic review. *Rev Panam Salud Pública*. 2019;43:1.
67. Shah MD, Iqbal M. Diazinon-induced oxidative stress and renal dysfunction in rats. *Food Chem Toxicol*. 2010;48:3345–3353.
68. Tripathi S, Srivastav AK. Nephrotoxicity induced by long-term oral administration of different doses of chlorpyrifos. *Toxicol Ind Heal*. 2010;26:439–447.
69. Rankin GO, Racine C, Sweeney A, et al. In vitro nephrotoxicity induced by Propanil. *Environ Toxicol*. 2008;2:435–442.
70. Baldi I, Lebailly P, Rondeau V, et al. Levels and determinants of pesticide exposure in operators involved in treatment of vineyards: results of the PESTEXPO Study. *J Expo Sci Environ Epidemiol*. 2012;22:593–600.
71. Grgic I, Campanholle G, Bijol V, et al. Targeted proximal tubule injury triggers interstitial fibrosis and glomerulosclerosis. *Kidney Int*. 2012;82:172–183.
72. Fischer RSB, Vangala C, Truong L, et al. Early detection of acute tubulointerstitial nephritis in the genesis of Mesoamerican nephropathy. *Kidney Int*. 2018;93:753–760.
73. Sabour MS, MacDonald MK, Lambie AT, et al. The electron microscopic appearance of the kidney in hydrated and dehydrated rats. *Q J Exp Physiol Cogn Med Sci*. 1963;49:162–170.
74. Nouwen EJ, Verstrepen WA, Buyssens N, et al. Hyperplasia, hypertrophy, and phenotypic alterations in the distal nephron after acute proximal tubular injury in the rat. *Lab Invest*. 1994;70:479–493.
75. Schindelin J, Arganda-Carreras I, Frise E, et al. Fiji: an open-source platform for biological-image analysis. *Nat Methods*. 2012;9:676–682.